

Enforcing Statistical Orthogonality in Massive MIMO Systems via Covariance Shaping

Placido Mursia *Student Member, IEEE*, Italo Atzeni, *Member, IEEE*,
 Laura Cottatellucci, *Member, IEEE*, and David Gesbert, *Fellow, IEEE*

Abstract

This paper tackles the problem of downlink transmission in massive multiple-input multiple-output (MIMO) systems where the equipments (UEs) exhibit high spatial correlation and the channel estimation is limited by strong pilot contamination. Signal subspace separation among the UEs is, in fact, rarely realized in practice and is generally beyond the control of the network designer (as it is dictated by the physical scattering environment). In this context, we propose a novel statistical beamforming technique, referred to as *MIMO covariance shaping*, that exploits multiple antennas at the UEs and leverages the realistic non-Kronecker structure of massive MIMO channels to target a suitable shaping of the channel statistics performed at the UE-side. To optimize the covariance shaping strategies, we propose a low-complexity block coordinate descent algorithm that is proved to converge to a limit point of the original nonconvex problem. For the two-UE case, this is shown to converge to a stationary point of the original problem. Numerical results illustrate the sum-rate performance gains of the proposed method with respect to reference scenarios employing the multiple antennas at the UE for spatial multiplexing.

***Index terms*—Covariance shaping, massive MIMO, multi-user MIMO, pilot contamination, statistical beamforming.**

P. Mursia is with the Communication Systems Department, EURECOM, France and with NEC Laboratories Europe GmbH, Heidelberg, Germany (email: placido.mursia@neclab.eu). I. Atzeni is with the Centre for Wireless Communications, University of Oulu, Finland (email: italo.atzeni@oulu.fi). L. Cottatellucci is with the Department of Electrical, Electronics, and Communication Engineering, Friedrich-Alexander University Erlangen-Nuremberg, Germany (email: laura.cottatellucci@fau.de). D. Gesbert is with the Communication Systems Department, EURECOM, France (email: david.gesbert@eurecom.fr).

The work of P. Mursia was supported by the Marie Skłodowska-Curie Actions (MSCA-ITN 722788 SPOTLIGHT). The work of I. Atzeni was supported by the Marie Skłodowska-Curie Actions (MSCA-IF 897938 DELIGHT). Part of this work has been presented at IEEE GLOBECOM 2018 [1] and at IEEE CAMAD 2018 [2].

I. INTRODUCTION

Massive multiple-input multiple-output (MIMO) is a multi-antenna technology that has a great potential to boost the spectral efficiency (SE) of cellular networks by means of highly directional beamforming and spatial multiplexing of many user equipments (UEs) in the same time-frequency resources. It thus plays a pivotal role in current fifth-generation (5G) implementations [3]–[5] and is expected to maintain this prominence in future wireless generations [6]–[10]. The benefits of massive MIMO can be ascribed to the large number of antennas available at the base station (BS), which we denote by M . Indeed, by means of coherent combination of the transmit signals, the useful power at the receiver is increased by a factor of M compared with the case of single-antenna transmitter. However, such a coherent transmission requires the availability of instantaneous channel state information at the transmitter (CSIT), which poses several challenges in terms of system design.

The acquisition of the channel state information (CSI) vectors associated with each UE has a high cost in terms of signaling overhead and computational complexity due to the high dimensionality of the massive MIMO channels. Specifically, it implies allocating considerable communication resources to pilot-aided channel estimation and involves large matrix operations in the precoding/decoding design. In frequency-division duplex (FDD) systems, the CSI is obtained via downlink pilots and the signaling overhead scales with the number of BS antennas M , which becomes impractical as M grows large [11]. In contrast, in time-division duplex (TDD) systems, the CSI is acquired by means of uplink pilots exploiting channel reciprocity and the signaling overhead scales with the number of UEs K . However, since the channel coherence time is limited, the same pilots must be reused across different UEs, thus generating pilot contamination that greatly reduces the quality of the CSI and may compromise the network performance [12], [13]. In [14], it was shown that the achievable SE of massive MIMO systems is not limited by pilot contamination when multi-cell minimum mean squared error (MMSE) precoding is adopted. Nevertheless, this approach requires sharing the CSI across all the cells, which sensibly increases the overall signaling overhead.

To overcome such issues and facilitate the operations in the massive MIMO regime, several works have proposed to leverage statistical CSI [1], [2], [11], [15]–[25]. This consists mainly in the channel covariance matrix of each UE, which is essentially dictated by the angle spread spanned by the multipath propagation of the signals impinging on the antenna array. This angle

spread is often bounded due to the high spatial resolution of the massive array compared with the limited scattering environment. As a result, the channel covariance matrices in massive MIMO tend to be low-rank and dominated by few major propagation directions [14]–[16], [19]. This particular property can be exploited for several applications such as reducing the feedback overhead in the channel estimation phase [11], [19], [20] and mitigating the interference in the downlink data transmission phase when the UEs exhibit non-overlapping or orthogonal signal subspaces [15], [16]. For example, statistical CSI can be used to precode signals such that their chosen propagation paths do not interfere on average [17], [18]. In this regard, a robust precoding/decoding design based on the average mean squared error (MSE) matrix under different CSI conditions is derived in [17]. Furthermore, [18] provides a lower bound on the ergodic sum rate for the two-UE setting when the UEs are equipped with a single antenna.

There is a large body of literature focusing on the hybrid precoding problem, where the beamforming applied at the BS is divided into inner and outer precoding matrices [11], [19]–[22]. Here, the former is based on instantaneous CSI while the latter depends only on the second-order channel statistics. This results in reduced pilot length required for the instantaneous effective channel estimation and lower computational complexity associated with the inner precoding design. Moreover, in the context of FDD systems, such a hybrid precoding method can be used to reduce the size of the resulting effective channels by exploiting the near-orthogonality of the angle spreads of different UE groups [11]. In [19], this approach is shown to incur no loss compared with the full CSIT case when the number of BS antennas grows large, while the same scaling is obtained in [20] for the case of finite number of BS antennas and suitable UE scheduling. In TDD systems, existing works have pointed out how the exploitation of statistical CSI enables efficient pilot reuse across the UEs [15], [23]–[25]. In [23], pilot reuse for massive MIMO transmissions over spatially correlated Rayleigh fading channels is proposed when the angle spreads of the UEs with the same pilots are non-overlapping. In [24], the second-order channel statistics are used to precode the pilots, thus reducing the variance of the channel estimation error by a factor that is proportional to the number of antennas at the UEs. A robust channel estimation method coping with scenarios in which the angle spreads of the desired and interfering channels are overlapping is proposed in [25] and exploits channel separability in the power domain [26].

Most of the above works rely on a specific structure of the channel covariance matrices of the UEs in terms of rank and degree of separation among the signal subspaces. Such properties

are determined by the positions of the UEs combined with the physical scattering environment, where both these factors are generally beyond the control of the network designer. Indeed, in many practical scenarios, the UEs exhibit high spatial correlation, e.g., when they are not sufficiently far apart. Hence, the condition of non-overlapping or orthogonal signal subspaces is rarely satisfied in practice [14]. Moreover, existing works are often based on the assumption of Kronecker channel model, owing to its simple analytical formulation. However, such a model has been shown to be an over-simplification of the true nature of the MIMO channel [27].

A. Contributions

Building on the fact that most current and future UEs are, and will be, equipped with a small-to-moderate number of antennas, this paper proposes a novel statistical beamforming technique at the UEs-side, referred to as *MIMO covariance shaping*.¹ While existing methods assume statistical orthogonality among the UEs as a property given by the physical scattering environment and the Kronecker channel model due to its analytical tractability, MIMO covariance shaping aims at modifying the channel statistics of the UEs in order to enforce signal subspace separation in any given network scenario. The proposed approach targets a suitable shaping of the covariance matrix performed at the UE-side and relies uniquely on statistical CSI. Specifically, it consists in preemptively applying a statistical beamforming at each UE during both the uplink pilot-aided channel estimation phase and the downlink data transmission phase to enforce a separation of the signal subspaces of UEs that would be otherwise highly overlapping. In this context, each UE exploits its antennas to excite only a subset of all the possible propagation directions towards the BS such that the spatial correlation among the interfering UEs is minimized while preserving enough useful power for effective data transmission. Hence, MIMO covariance shaping is suitable for both pilot decontamination in TDD systems and statistical precoding. Remarkably, the proposed method exploits the realistic non-Kronecker channel structure, which allows to suitably alter the channel statistics perceived at the BS by designing the transceiver at the UE-side. Therefore, it has the unique advantage of turning the generally inconvenient non-Kronecker nature of massive MIMO channels into a benefit. Numerical results show the sum-rate performance gains with respect to reference schemes employing the multiple antennas

¹Note that the term “covariance shaping” has been used in the past in different contexts, mainly estimation theory (see, e.g., [28]).

at the UE for spatial multiplexing in scenarios where the UEs have highly overlapping covariance matrices and the channel estimation is limited by strong pilot contamination.

The MIMO covariance shaping framework was initially proposed in our prior works [1], [2] and recently used for the minimization of the outage probability in [29]. In this work, the authors extend the metric proposed in [1] to all pairs of interfering UEs to design a statistical receive beamforming at the UE along with a statistical precoding at the BS. Differently from [29], we argue that MIMO covariance shaping must be adopted for *both* pilot decontamination during the uplink pilot-aided channel estimation phase and receive combining during the downlink data transmission phase. By doing so, the BS is able to acquire accurate instantaneous estimates of the effective channels, which are then used for efficient downlink precoding and result in a great enhancement of the network performance.

The contributions of this paper are summarized as follows.

- We present the novel concept of MIMO covariance shaping, which aims at designing a suitable shaping of the covariance matrices of the UEs to enforce a full or partial separation of their signal subspaces, which would be otherwise highly overlapping.
- We point out that the exploitation of the non-Kronecker nature of massive MIMO channels is crucial to suitably alter the channel statistics perceived at the BS by acting at the UE-side.
- We derive a tractable expression of the ergodic achievable sum rate under MIMO covariance shaping with the objective of characterizing the impact of the proposed framework on the system performance.
- We optimize the covariance shaping strategies by minimizing the variance of the inter-UE interference (as a metric to measure the spatial correlation) among the interfering UEs. To this end, we propose a low-complexity block coordinate descent algorithm that is proved to converge to a limit point of the original nonconvex problem. For the two-UE case, this is shown to converge to a stationary point of the original problem.
- We provide numerical results that highlight the superior sum-rate performance of MIMO covariance shaping with respect to reference schemes where the multiple antennas at the UE are employed for spatial multiplexing in scenarios where the UEs exhibit high spatial correlation.

Outline. The rest of the paper is structured as follows. Section II introduces the system model for a general multi-UE MIMO downlink system. Section III presents the concept of MIMO covariance shaping. Section IV proposes efficient methods to optimize the covariance

shaping vectors. Section V presents numerical results to evaluate the performance of the proposed framework. Finally, Section VI concludes the paper.

Notation. Lowercase and uppercase boldface letters denote vectors and matrices, respectively, whereas $(\cdot)^T$, $(\cdot)^H$, and $(\cdot)^*$ are the transpose, Hermitian transpose, and conjugate operators, respectively. $\|\cdot\|$ and $\|\cdot\|_F$ represent the Euclidean norm for vectors and the Frobenius norm for matrices, respectively, whereas $\mathbb{E}[\cdot]$ and $\mathbb{V}[\cdot]$ are the expectation and variance operators, respectively. \mathbf{I}_A denotes the A -dimensional identity matrix and $\mathbf{0}$ represents the zero vector or matrix with proper dimension. $\text{tr}(\cdot)$ and $\text{vec}(\cdot)$ are the trace and vectorization operators, respectively. $(a_{mn})_{m,n=1}^M$ denotes the matrix of size $M \times M$ whose (m, n) th element is given by a_{mn} , whereas $[a_1, \dots, a_A]$ represents horizontal concatenation. We use \otimes to denote the Kronecker product and $\mathbf{u}_{\min}(\mathbf{A})$ to denote the eigenvector corresponding to the minimum eigenvalue of matrix \mathbf{A} , with $\|\mathbf{u}_{\min}(\mathbf{A})\| = 1$. $\mathbb{1}_{\mathcal{A}}(i, j)$ denotes the indicator function, which is equal to 1 if both i and j belong to set \mathcal{A} and to 0 otherwise, and $\lceil \cdot \rceil$ is the ceiling operator. Lastly, $\mathcal{CN}(\mathbf{0}, \mathbf{A})$ is the circularly symmetric complex Gaussian distribution with zero mean and covariance matrix \mathbf{A} .

II. SYSTEM MODEL

In this section, we introduce the channel model for a general multi-UE MIMO downlink system. Then, using the property of channel reciprocity between the uplink and the downlink, we present the channel estimation based on uplink pilot transmission. Finally, we discuss the system model for the data transmission in the downlink.

A. Channel Model

Consider a multi-UE MIMO system where a BS equipped with M antennas serves K UEs with N antennas each in the downlink. Let $\mathbf{H}_k \triangleq [\mathbf{h}_{k,1}, \dots, \mathbf{h}_{k,M}] = [\mathbf{g}_{k,1}^T, \dots, \mathbf{g}_{k,N}^T]^T \in \mathbb{C}^{N \times M}$ denote the downlink channel matrix of UE k , where $\mathbf{h}_{k,m} \in \mathbb{C}^{N \times 1}$ and $\mathbf{g}_{k,n} \in \mathbb{C}^{1 \times M}$ are the channel vectors between the m th BS antenna and UE k and between the BS and the n th antenna of UE k , respectively. We assume a general channel model where the entries of \mathbf{H}_k satisfy $\text{vec}(\mathbf{H}_k) \sim \mathcal{CN}(\mathbf{0}, \mathbf{\Sigma}_k)$ [30, Ch. 3]. Here, the covariance matrix $\mathbf{\Sigma}_k \in \mathbb{C}^{NM \times NM}$ has the

following general structure:

$$\boldsymbol{\Sigma}_k \triangleq \begin{bmatrix} \boldsymbol{\Sigma}_{k,11} & \boldsymbol{\Sigma}_{k,12} & \cdots & \boldsymbol{\Sigma}_{k,1M} \\ \boldsymbol{\Sigma}_{k,12}^H & \boldsymbol{\Sigma}_{k,22} & & \vdots \\ \vdots & & \ddots & \\ \boldsymbol{\Sigma}_{k,1M}^H & \cdots & & \boldsymbol{\Sigma}_{k,MM} \end{bmatrix} \quad (1)$$

where each block $\boldsymbol{\Sigma}_{k,mn} \triangleq \mathbb{E}[\mathbf{h}_{k,m} \mathbf{h}_{k,n}^H] \in \mathbb{C}^{N \times N}$ represents the cross-covariance matrix between the m th and n th columns of \mathbf{H}_k . Lastly, we define the covariance matrix seen at UE k as $\mathbf{R}_k \triangleq \mathbb{E}[\mathbf{H}_k \mathbf{H}_k^H] \in \mathbb{C}^{N \times N}$ and the covariance matrix relative to UE k seen at the BS as $\mathbf{T}_k \triangleq \mathbb{E}[\mathbf{H}_k^H \mathbf{H}_k] \in \mathbb{C}^{M \times M}$, respectively. Observe that, in the case of downlink transmission, \mathbf{R}_k and \mathbf{T}_k represent the receive and transmit covariance matrices, respectively.

B. Uplink Pilot-Aided Channel Estimation

Assuming a TDD setting and channel reciprocity between the uplink and the downlink (see, e.g., [31]), the channel matrices $\{\mathbf{H}_k\}_{k=1}^K$ are estimated at the BS via antenna-specific uplink pilots, such that N pilot vectors per UE are required. Let $\mathcal{S}_p \triangleq \{k : \text{UE } k \text{ has pilot } \mathbf{P}_p\}$ be the set of UEs sharing the same pilot matrix $\mathbf{P}_p \in \mathbb{C}^{N \times \tau}$, with $p = 1, \dots, P$. Here, $P < K$ denotes the number of orthogonal pilot matrices and τ represents the pilot length. The orthogonal pilot matrices satisfy $\{\mathbf{P}_p \mathbf{P}_p^H = \frac{\tau}{N} \mathbf{I}_N\}_{p=1}^P$, i.e., N orthogonal pilot vectors are assigned to each UE, and $\{\mathbf{P}_p \mathbf{P}_q^H = \mathbf{0}\}_{p \neq q}$: note that these conditions imply $\tau \geq PN$. Furthermore, $\mathbf{Y} \in \mathbb{C}^{M \times \tau}$ denotes the receive signal at the BS during the uplink pilot-aided channel estimation phase, which is given by

$$\mathbf{Y} \triangleq \sum_{p=1}^P \sum_{k \in \mathcal{S}_p} \sqrt{\rho_{\text{UE}}} \mathbf{H}_k^H \mathbf{P}_p + \mathbf{Z} \quad (2)$$

where ρ_{UE} is the transmit power at the UEs and $\mathbf{Z} \in \mathbb{C}^{M \times \tau}$ is the noise term at the BS with elements distributed independently as $\mathcal{CN}(0, \sigma_{\text{BS}}^2)$. Let $\boldsymbol{\Phi}_{k,nn} \triangleq \mathbb{E}[\mathbf{g}_{k,n}^T \mathbf{g}_{k,n}^*]$ denote the covariance matrix of $\mathbf{g}_{k,n}$. Then, the MMSE estimate of $\mathbf{g}_{k,n}$, with $k \in \mathcal{S}_p$, is given by (see, e.g., [14])

$$\hat{\mathbf{g}}_{k,n}^H \triangleq \frac{N}{\tau \sqrt{\rho_{\text{UE}}}} \boldsymbol{\Phi}_{k,nn} \mathbf{Q}_{k,nn}^{-1} \mathbf{Y} \mathbf{P}_p^H \mathbf{e}_n \quad (3)$$

where $\mathbf{e}_n \in \mathbb{R}^{N \times 1}$ is the n th column of \mathbf{I}_N , $\mathbf{Q}_{k,nn} \triangleq (\boldsymbol{\Phi}_{k,nn} + \sum_{j \in \mathcal{S}_p \setminus \{k\}} \boldsymbol{\Phi}_{j,nn} + \frac{N}{\tau \rho_{\text{UE}}} \mathbf{I}_M)$ is the normalized covariance of the receive signal after correlating with $\mathbf{P}_p^H \mathbf{e}_n$, and $\rho_{\text{UE}} \triangleq \frac{\rho_{\text{UE}}}{\sigma_{\text{BS}}^2}$ is

the transmit signal-to-noise ratio (SNR) at the UEs. Finally, the estimate of \mathbf{H}_k is obtained as $\hat{\mathbf{H}}_k \triangleq [\hat{\mathbf{g}}_{k,1}^T, \dots, \hat{\mathbf{g}}_{k,N}^T]^T$.

C. Downlink Data Transmission

In the following, we focus on the downlink data transmission and assume that the BS transmits L_k independent symbols to UE k . We denote the transmit symbol vector for UE k by $\mathbf{s}_k \in \mathbb{C}^{L_k \times 1}$, with $\mathbb{E}[\mathbf{s}_k \mathbf{s}_k^H] = \mathbf{I}_{L_k}$, and introduce the multi-UE transmit symbol vector $\mathbf{s} \triangleq [\mathbf{s}_1^T, \dots, \mathbf{s}_K^T]^T \in \mathbb{C}^{L \times 1}$, with $L \triangleq \sum_{k=1}^K L_k$. Before the transmission, the BS precodes \mathbf{s} using the multi-UE precoding matrix $\mathbf{W} \triangleq [\mathbf{W}_1, \dots, \mathbf{W}_K] \in \mathbb{C}^{M \times L}$, where $\mathbf{W}_k \triangleq [\mathbf{w}_{k,1}, \dots, \mathbf{w}_{k,L_k}] \in \mathbb{C}^{M \times L_k}$ is the precoding matrix corresponding to \mathbf{s}_k and \mathbf{W} satisfies the power constrain $\|\mathbf{W}\|_F^2 = 1$. The receive signal at UE k is thus given by

$$\mathbf{y}_k \triangleq \sqrt{\rho_{\text{BS}}} \mathbf{H}_k \mathbf{W} \mathbf{s} + \mathbf{z}_k \quad (4)$$

$$= \sqrt{\rho_{\text{BS}}} \mathbf{H}_k \mathbf{W}_k \mathbf{s}_k + \sqrt{\rho_{\text{BS}}} \sum_{j \neq k} \mathbf{H}_k \mathbf{W}_j \mathbf{s}_j + \mathbf{z}_k \quad (5)$$

where ρ_{BS} is the transmit power at the BS and $\mathbf{z}_k \sim \mathcal{CN}(0, \sigma_{\text{UE}}^2 \mathbf{I}_N)$ is the noise term at the UEs. Finally, UE k decodes \mathbf{s}_k as $\hat{\mathbf{s}}_k \triangleq \mathbf{V}_k^H \mathbf{y}_k$, where $\mathbf{V}_k \triangleq [\mathbf{v}_{k,1}, \dots, \mathbf{v}_{k,L_k}] \in \mathbb{C}^{N \times L_k}$ is the corresponding combining matrix. The resulting sum rate is given by

$$R \triangleq \sum_{k=1}^K \sum_{\ell=1}^{L_k} \log_2 \left(1 + \frac{|\mathbf{v}_{k,\ell}^H \mathbf{H}_k \mathbf{w}_{k,\ell}|^2}{\sum_{(j,s) \neq (k,\ell)} |\mathbf{v}_{k,\ell}^H \mathbf{H}_k \mathbf{w}_{j,s}|^2 + \frac{1}{\varrho_{\text{BS}}} \|\mathbf{v}_{k,\ell}\|^2} \right) \quad (6)$$

with $\varrho_{\text{BS}} \triangleq \frac{\rho_{\text{BS}}}{\sigma_{\text{UE}}^2}$ being the transmit SNR at the BS.

III. COVARIANCE SHAPING AT THE UE-SIDE

In a massive MIMO setting, the BS can spatially separate signals corresponding to different UEs and mitigate or eliminate the pilot contamination if their covariance matrices lie on orthogonal supports, i.e., if $\Sigma_k \Sigma_j = \mathbf{0}$ for a given pair of UEs k and j . However, the degree of statistical orthogonality between UEs is determined by their positions combined with the surrounding physical scattering environment and both these factors are generally beyond the control of network designers. Hence, signal subspace separation among the UEs rarely occurs in practice [14]. In this context, we propose a novel method relying uniquely on statistical CSI and referred to as *MIMO covariance shaping* (or, for simplicity, *covariance shaping*), which is applied at the UE-side to enforce the aforementioned signal subspace separation in any given

network scenario. According to covariance shaping, the UEs preemptively apply a statistical transmit/receive beamforming vector, different for each UE, that aims at spatially separating their transmissions, thus drastically reducing both pilot contamination and interference. Here, the original MIMO channel of each UE is transformed into an effective multiple-input single-output (MISO) channel by combining the transmit/receive signal with the corresponding covariance shaping vector. Remarkably, the proposed method exploits the realistic non-Kronecker structure of massive MIMO channels that allows to suitably alter the channel statistics perceived at the BS by acting at the UE-side, thus turning a generally inconvenient model into a benefit.

Let $\mathbf{v}_k \in \mathbb{C}^{N \times 1}$ denote the statistical beamforming vector preemptively applied by UE k : in the rest of the paper, we refer to \mathbf{v}_k as *covariance shaping vector*. Hence, the MIMO channel \mathbf{H}_k between the BS and each UE k is transformed into the effective MISO channel $\bar{\mathbf{g}}_k \triangleq \mathbf{v}_k^H \mathbf{H}_k \in \mathbb{C}^{1 \times M}$. In this setting, it follows that $\bar{\mathbf{g}}_k \sim \mathcal{CN}(\mathbf{0}, \bar{\Phi}_k)$, where $\bar{\Phi}_k \in \mathbb{C}^{M \times M}$ is the effective covariance matrix defined as

$$\bar{\Phi}_k \triangleq \mathbb{E}[\bar{\mathbf{g}}_k^T \bar{\mathbf{g}}_k^*] \quad (7)$$

$$= ((\mathbf{I}_M \otimes \mathbf{v}_k^H) \Sigma_k (\mathbf{I}_M \otimes \mathbf{v}_k))^T \quad (8)$$

with Σ_k introduced in (1) and where $\mathbb{E}[|\bar{\mathbf{g}}_k|^2] = \text{tr}(\bar{\Phi}_k)$. In the rest of this section, we describe how the two phases of uplink pilot-aided channel estimation and downlink data transmission are modified under covariance shaping and we provide a tractable expression of the resulting ergodic achievable sum rate. The optimization of the covariance shaping vectors is discussed in Section IV.

A. Uplink Pilot-Aided Channel Estimation

To estimate the effective channels $\{\bar{\mathbf{g}}_k\}_{k=1}^K$ resulting from covariance shaping, the BS assigns the same pilot vector $\mathbf{p}_p \in \mathbb{C}^{1 \times \tau}$ to all UEs $k \in \mathcal{S}_p$, with $\{\|\mathbf{p}_p\|^2 = \tau\}_{p=1}^P$ and $\{\mathbf{p}_p \mathbf{p}_q^H = 0\}_{p \neq q}$. The receive signal at the BS during the uplink pilot-aided channel estimation phase, which we denote by $\bar{\mathbf{Y}} \in \mathbb{C}^{M \times \tau}$, is given by (cf. (2))

$$\bar{\mathbf{Y}} \triangleq \sum_{p=1}^P \sum_{k \in \mathcal{S}_p} \sqrt{\rho_{\text{UE}}} \bar{\mathbf{g}}_k^H \mathbf{p}_p + \mathbf{Z}. \quad (9)$$

Then, the MMSE estimate of $\bar{\mathbf{g}}_k$, with $k \in \mathcal{S}_p$, is given by (cf. (3))

$$\hat{\bar{\mathbf{g}}}_k^H \triangleq \frac{1}{\tau \sqrt{\rho_{\text{UE}}}} \bar{\Phi}_k \mathbf{Q}_k^{-1} \bar{\mathbf{Y}} \mathbf{p}_p^H \quad (10)$$

where $\mathbf{Q}_k \triangleq \bar{\Phi}_k + \sum_{j \in \mathcal{S}_p \setminus \{k\}} \bar{\Phi}_j + \frac{1}{\tau \rho_{\text{UE}}} \mathbf{I}_M \in \mathbb{C}^{M \times M}$ is the normalized covariance of the receive signal after correlating with \mathbf{p}_p^H . Note that the estimation of the effective channels only requires one pilot vector per UE. Hence, the application of covariance shaping can potentially reduce the pilot length with respect to the estimation of the channel matrices $\{\mathbf{H}_k\}_{k=1}^K$ described in Section II-B, which requires N pilot vectors per UE.

B. Downlink Data Transmission

Focusing on the downlink data transmission, the BS now transmits only one symbol $s_k \in \mathbb{C}$ to each UE k , i.e., $\{L_k = 1\}_{k=1}^K$. Hence, we have $\mathbf{s} = [s_1, \dots, s_K]^T \in \mathbb{C}^{K \times 1}$ and the multi-UE precoding matrix becomes $\mathbf{W} = [\mathbf{w}_1, \dots, \mathbf{w}_K] \in \mathbb{C}^{M \times K}$, where $\mathbf{w}_k \in \mathbb{C}^{M \times 1}$ is the precoding vector corresponding to s_k . The receive signal at UE k is thus given by (cf. (4)–(5))

$$\bar{y}_k \triangleq \sqrt{\rho_{\text{BS}}} \bar{\mathbf{g}}_k \mathbf{W} \mathbf{s} + \mathbf{v}_k^H \mathbf{z}_k \quad (11)$$

$$= \sqrt{\rho_{\text{BS}}} \bar{\mathbf{g}}_k \mathbf{w}_k s_k + \sqrt{\rho_{\text{BS}}} \sum_{j \neq k} \bar{\mathbf{g}}_k \mathbf{w}_j s_j + \mathbf{v}_k^H \mathbf{z}_k \quad (12)$$

and the resulting sum rate is given by (cf. (6))

$$\bar{R} \triangleq \sum_{k=1}^K \log_2 \left(1 + \frac{|\bar{\mathbf{g}}_k \mathbf{w}_k|^2}{\sum_{j \neq k} |\bar{\mathbf{g}}_k \mathbf{w}_j|^2 + \frac{1}{\rho_{\text{BS}}} \|\mathbf{v}_k\|^2} \right). \quad (13)$$

C. Ergodic Achievable Sum Rate

We now analyze the sum rate as a function of the covariance shaping vectors with the objective of characterizing the impact of the proposed framework on the system performance. In particular, we derive a tractable expression of the ergodic achievable sum rate by assuming that each UE k does not know the effective scalar channel $\bar{\mathbf{g}}_k \mathbf{w}_k = \mathbf{v}_k^H \mathbf{H}_k \mathbf{w}_k$ instantaneously but only its expected value. Building on the results in [12]–[14], [32], we can express the receive signal in (12) as

$$\bar{y}_k = \sqrt{\rho_{\text{BS}}} \mathbb{E}[\bar{\mathbf{g}}_k \mathbf{w}_k] s_k + \sqrt{\rho_{\text{BS}}} (\bar{\mathbf{g}}_k \mathbf{w}_k - \mathbb{E}[\bar{\mathbf{g}}_k \mathbf{w}_k]) s_k + \sqrt{\rho_{\text{BS}}} \sum_{j \neq k} \bar{\mathbf{g}}_k \mathbf{w}_j s_j + \mathbf{v}_k^H \mathbf{z}_k \quad (14)$$

$$= \sqrt{\rho_{\text{BS}}} \mathbb{E}[\bar{\mathbf{g}}_k \mathbf{w}_k] s_k + z'_k \quad (15)$$

where the effective noise term $z'_k \triangleq \sqrt{\rho_{\text{BS}}}(\bar{\mathbf{g}}_k \mathbf{w}_k - \mathbb{E}[\bar{\mathbf{g}}_k \mathbf{w}_k])s_k + \sqrt{\rho_{\text{BS}}} \sum_{j \neq k} \bar{\mathbf{g}}_k \mathbf{w}_j s_j + \mathbf{v}_k^H \mathbf{z}_k$ accounts for the lack of instantaneous CSIT in addition to the interference and the noise at UE k . Hence, we define the *effective* signal-to-interference-plus-noise ratio (SINR) at UE k as

$$\gamma_k \triangleq \frac{|\mathbb{E}[\bar{\mathbf{g}}_k \mathbf{w}_k]|^2}{\mathbb{V}[\bar{\mathbf{g}}_k \mathbf{w}_k] + \sum_{j \neq k} \mathbb{E}[|\bar{\mathbf{g}}_k \mathbf{w}_j|^2] + \frac{1}{\rho_{\text{BS}}} \|\mathbf{v}_k\|^2} \quad (16)$$

which is obtained by assuming the worst-case scenario of Gaussian-distributed effective noise z'_k .

The expression in (16) can be further simplified by considering the case where the BS adopts maximum ratio transmission (MRT) precoding. In this setting, the multi-UE precoding matrix can be written as

$$\mathbf{W} = \frac{\hat{\mathbf{H}}^H}{\sqrt{\mathbb{E}[\|\hat{\mathbf{H}}\|_F^2]}} \quad (17)$$

where $\bar{\mathbf{H}} \triangleq [\bar{\mathbf{g}}_1^T, \dots, \bar{\mathbf{g}}_K^T]^T \in \mathbb{C}^{K \times M}$ and $\hat{\mathbf{H}} \triangleq [\hat{\mathbf{g}}_1^T, \dots, \hat{\mathbf{g}}_K^T]^T \in \mathbb{C}^{K \times M}$ contain the effective channels and their MMSE estimates defined in (10), respectively. Hence, when MRT precoding is adopted at the BS, the effective SINR in (16) reduces to

$$\gamma_k = \frac{|\mathbb{E}[\bar{\mathbf{g}}_k \hat{\mathbf{g}}_k^H]|^2}{\mathbb{V}[\bar{\mathbf{g}}_k \hat{\mathbf{g}}_k^H] + \sum_{j \neq k} \mathbb{E}[|\bar{\mathbf{g}}_k \hat{\mathbf{g}}_j^H|^2] + \frac{1}{\rho_{\text{BS}}} \|\mathbf{v}_k\|^2 \mathbb{E}[\|\bar{\mathbf{H}}\|_F^2]} \quad (18)$$

$$= \frac{\text{tr}(\bar{\Phi}_k \mathbf{Q}_k^{-1} \bar{\Phi}_k)^2}{\sum_{j=1}^K \text{tr}(\bar{\Phi}_k \bar{\Phi}_j \mathbf{Q}_j^{-1} \bar{\Phi}_j) + \sum_{j \neq k} \mathbb{1}_{S_p}(k, j) \text{tr}(\bar{\Phi}_k \mathbf{Q}_j^{-1} \bar{\Phi}_j)^2 + \frac{1}{\rho_{\text{BS}}} \|\mathbf{v}_k\|^2 \sum_{j=1}^K \text{tr}(\bar{\Phi}_j)} \quad (19)$$

where (19) results from plugging the following terms into (18): $\mathbb{E}[\bar{\mathbf{g}}_k \hat{\mathbf{g}}_k^H] = \text{tr}(\bar{\Phi}_k \mathbf{Q}_k^{-1} \bar{\Phi}_k)$, $\mathbb{V}[\bar{\mathbf{g}}_k \hat{\mathbf{g}}_k^H] = \text{tr}(\bar{\Phi}_k^2 \mathbf{Q}_k^{-1} \bar{\Phi}_k)$, $\mathbb{E}[|\bar{\mathbf{g}}_k \hat{\mathbf{g}}_j^H|^2] = \text{tr}(\bar{\Phi}_k \bar{\Phi}_j \mathbf{Q}_j^{-1} \bar{\Phi}_j) + \mathbb{1}_{S_p}(k, j) \text{tr}(\bar{\Phi}_k \mathbf{Q}_j^{-1} \bar{\Phi}_j)^2$, and $\mathbb{E}[\|\bar{\mathbf{H}}\|_F^2] = \sum_{k=1}^K \text{tr}(\bar{\Phi}_k)$. We refer to Appendix I for the detailed derivations. Note that, in the case of perfect channel estimation, i.e., when $\rho_{\text{UE}} \rightarrow \infty$ and all the UEs have orthogonal pilots, we have $\{\bar{\Phi}_k \mathbf{Q}_k^{-1} \bar{\Phi}_k = \bar{\Phi}_k\}_{k=1}^K$ and $\{\mathbb{1}_{S_p}(k, j) = 0\}_{j \neq k}$. In this context, the effective SINR in (19) simplifies as

$$\gamma_k = \frac{\text{tr}(\bar{\Phi}_k)^2}{\sum_{j=1}^K \text{tr}(\bar{\Phi}_k \bar{\Phi}_j) + \frac{1}{\rho_{\text{BS}}} \|\mathbf{v}_k\|^2 \sum_{j=1}^K \text{tr}(\bar{\Phi}_j)}. \quad (20)$$

Finally, Proposition 1 presents expressions for the ergodic achievable sum rate in the two cases of perfect and imperfect channel estimation and in asymptotic conditions when the number of transmit antennas at the BS tends to infinity. The proof follows from [13, Sec. C] and is thus omitted.

Proposition 1. Assume that the BS adopts MRT precoding. Then, an ergodic achievable sum rate is given by

$$\bar{R}^{\text{lb}} = \sum_{k=1}^K \log_2(1 + \gamma_k) \quad (21)$$

with γ_k defined in (19) for the case of imperfect channel estimation and in (20) for the case of perfect channel estimation. Furthermore, the following limit holds as $M \rightarrow \infty$:

$$\lim_{M \rightarrow \infty} \bar{R}^{\text{lb}} = \mathbb{E}[\bar{R}] \quad (22)$$

with \bar{R} defined in (13).

IV. COVARIANCE SHAPING OPTIMIZATION

In this section, we address the sum rate maximization through a proper design of the covariance shaping vectors at the UEs. To this end, we consider the variance of the inter-UE interference as a metric to measure the spatial correlation (or, in other words, the degree of statistical orthogonality) between two interfering UEs. In the following, we first consider the simple case of $K = 2$ and then extend the resulting analysis to the general case of $K \geq 2$.

Let us define the inter-UE interference between UEs k and j after applying covariance shaping as

$$\Omega(\mathbf{v}_k, \mathbf{v}_j) \triangleq \frac{\bar{\mathbf{g}}_k(\mathbf{v}_k) \bar{\mathbf{g}}_j^{\text{H}}(\mathbf{v}_j)}{\sqrt{\mathbb{E}[\|\bar{\mathbf{g}}_k(\mathbf{v}_k)\|^2] \mathbb{E}[\|\bar{\mathbf{g}}_j(\mathbf{v}_j)\|^2]}} \quad (23)$$

where the notation $\bar{\mathbf{g}}_k(\mathbf{v}_k)$ makes explicit the dependence of the effective channel $\bar{\mathbf{g}}_k$ on the corresponding covariance shaping vector \mathbf{v}_k . The effective channels of UEs k and j yield asymptotic *favorable propagation* if they satisfy [33]

$$\lim_{M \rightarrow \infty} \Omega(\mathbf{v}_k, \mathbf{v}_j) = 0. \quad (24)$$

For a practical number of BS antennas M , a meaningful performance metric is the variance of $\Omega(\mathbf{v}_k, \mathbf{v}_j)$, expressed as

$$\delta(\mathbf{v}_k, \mathbf{v}_j) \triangleq \mathbb{V}[\Omega(\mathbf{v}_k, \mathbf{v}_j)] \quad (25)$$

$$= \frac{\text{tr}(\bar{\Phi}_k(\mathbf{v}_k) \bar{\Phi}_j(\mathbf{v}_j))}{\text{tr}(\bar{\Phi}_k(\mathbf{v}_k)) \text{tr}(\bar{\Phi}_j(\mathbf{v}_j))} \quad (26)$$

where the notation $\bar{\Phi}_k(\mathbf{v}_k)$ makes explicit the dependence of the effective covariance matrix $\bar{\Phi}_k$ on the corresponding covariance shaping vector \mathbf{v}_k . Note that the terms in (26) can be written as

$$\text{tr}(\bar{\Phi}_k(\mathbf{v}_k)\bar{\Phi}_j(\mathbf{v}_j)) = \sum_{m,n=1}^M \mathbf{v}_k^H \Sigma_{k,mn} \mathbf{v}_k \mathbf{v}_j^H \Sigma_{j,nm} \mathbf{v}_j \quad (27)$$

$$= \sum_{m,n=1}^M \mathbf{v}_k^H \Sigma_{k,mn} \mathbf{v}_k \mathbf{v}_j^H \Sigma_{j,mn}^H \mathbf{v}_j, \quad (28)$$

$$\text{tr}(\bar{\Phi}_k(\mathbf{v}_k)) = \mathbf{v}_k^H \left(\sum_{m=1}^M \Sigma_{k,mm} \right) \mathbf{v}_k \quad (29)$$

where we recall that $\Sigma_{k,mn}$ represents the cross-covariance matrix between the m th and n th columns of the original channel \mathbf{H}_k , i.e., before applying covariance shaping, as defined in (1). Observe that $\delta(\mathbf{v}_k, \mathbf{v}_j) = 0$ implies $\bar{\Phi}_k \bar{\Phi}_j = \mathbf{0}$, i.e., that $\bar{\Phi}_k$ and $\bar{\Phi}_j$ lie on orthogonal supports [14]. Indeed, considering the eigenvalue decomposition of the effective covariance matrices, which may be written as $\{\bar{\Phi}_i = \mathbf{U}_i \mathbf{\Lambda}_i \mathbf{U}_i^H\}_{i \in \{k,j\}}$, the condition of statistical orthogonality is satisfied if $\mathbf{U}_k = \mathbf{U}_j$ and $\text{tr}(\mathbf{\Lambda}_k \mathbf{\Lambda}_j) = 0$, which implies the rank-deficiency of both $\bar{\Phi}_k$ and $\bar{\Phi}_j$. Clearly, in the general case, this imposes M^2 conditions whereas only $2N$ variables can be adjusted: this means that the resulting system of equations can be solved when $N \geq \frac{M^2}{2}$, which is generally not verified in practice since $M \gg KN$ in massive MIMO scenarios. Hence, since full signal subspace separation can rarely be achieved by simple transceiver design at the UE-side, it is of interest to minimize the spatial correlation between each pair of UEs.

A. Two-UE Case

In the two-UE case, i.e., for $K = 2$, the covariance shaping vectors of UEs k and j are computed by solving the optimization problem

$$\begin{aligned} & \underset{\{\mathbf{v}_k, \mathbf{v}_j\}}{\text{minimize}} && \delta(\mathbf{v}_k, \mathbf{v}_j) \\ & \text{subject to} && \|\mathbf{v}_k\|^2 = \|\mathbf{v}_j\|^2 = 1 \end{aligned} \quad (\text{P1})$$

with $\delta(\mathbf{v}_k, \mathbf{v}_j)$ defined in (26). Although problem (P1) is not convex in either \mathbf{v}_k or \mathbf{v}_j , it can be efficiently solved via alternating optimization, as proposed in [1]. Let us introduce the definition

$$\eta_{j,mn}(\mathbf{v}_j) \triangleq \frac{\mathbf{v}_j^H \Sigma_{j,mn} \mathbf{v}_j}{\mathbf{v}_j^H \left(\sum_{m=1}^M \Sigma_{j,mm} \right) \mathbf{v}_j}. \quad (30)$$

Algorithm 1 (Covariance shaping: Alternating optimization algorithm)

Data: $\mathbf{v}_k^{(0)}$, $\mathbf{v}_j^{(0)}$, Σ_k , Σ_j , and ϵ . Fix $n = 1$.

While $|\delta(\mathbf{v}_k^{(n)}, \mathbf{v}_j^{(n)}) - \delta(\mathbf{v}_k^{(n-1)}, \mathbf{v}_j^{(n-1)})| / \delta(\mathbf{v}_k^{(n)}, \mathbf{v}_j^{(n)}) > \epsilon$

(S.1) Given $\mathbf{v}_j^{(n-1)}$, compute $\{\eta_{j,mn}(\mathbf{v}_j^{(n-1)})\}_{m,n=1}^M$ as in (30).

(S.2) Compute $\mathbf{v}_k^{(n)}$ as in (32).

(S.3) Given $\mathbf{v}_k^{(n)}$, compute $\{\eta_{k,mn}(\mathbf{v}_k^{(n)})\}_{m,n=1}^M$ as in (30).

(S.4) Compute $\mathbf{v}_j^{(n)}$ as in (32).

End

(S.5) Fix $\mathbf{v}_k = \mathbf{v}_k^{(n)}$ and $\mathbf{v}_j = \mathbf{v}_j^{(n)}$.

The optimal covariance shaping vector of UE k for a given \mathbf{v}_j , denoted by \mathbf{v}_k^* , is obtained as

$$\mathbf{v}_k^* = \underset{\mathbf{v}_k : \|\mathbf{v}_k\|^2=1}{\operatorname{argmin}} \frac{\sum_{m,n=1}^M \mathbf{v}_k^H (\eta_{j,mn}(\mathbf{v}_j) \Sigma_{k,mn}) \mathbf{v}_k}{\mathbf{v}_k^H (\sum_{m=1}^M \Sigma_{k,mm}) \mathbf{v}_k}. \quad (31)$$

Since (31) is in the form of generalized Rayleigh quotient, it admits the solution

$$\mathbf{v}_k^* = \mathbf{u}_{\min} \left(\left(\sum_{m=1}^M \Sigma_{k,mm} \right)^{-1} \left(\sum_{m,n=1}^M \eta_{j,mn}(\mathbf{v}_j) \Sigma_{k,mn} \right) \right) \quad (32)$$

and the optimal covariance shaping vector of UE j for a given \mathbf{v}_k is obtained in a similar way. Hence, problem (P1) is solved by alternating the optimization between \mathbf{v}_k and \mathbf{v}_j until a predetermined convergence criterion is satisfied, e.g., until the difference between the values of the objective between consecutive iterations is sufficiently small. This scheme is formalized in Algorithm 1, whose convergence properties are characterized in Proposition 2.

Proposition 2. *The alternating optimization algorithm described in Algorithm 1 converges to a stationary point of problem (P1).*

Proof: Observe that the objective function in (31) does not depend on the scaling of \mathbf{v}_k and, if we relax the nonconvex constraint $\|\mathbf{v}_k\|^2 = 1$ as $\|\mathbf{v}_k\|^2 \leq 1$, (32) remains a solution of (31). Then, according to [34, Corollary 2], every limit point of the sequence generated by the alternating optimization algorithm applied to problem (P1) with the relaxed constraints is a stationary point of the original problem. ■

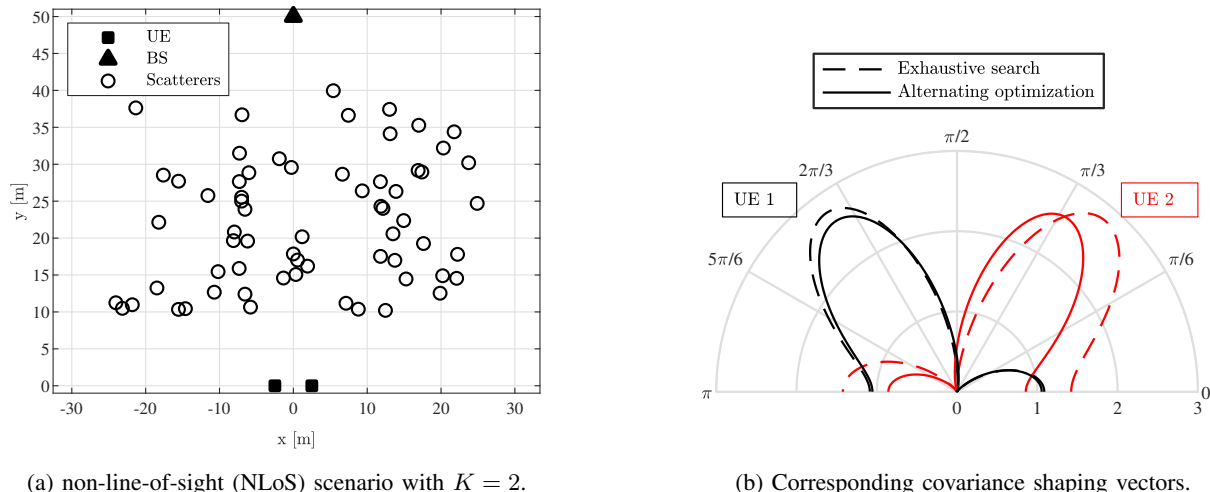


Fig. 1: (a) Map of the considered NLoS scenario with $K = 2$; (b) Corresponding covariance shaping vectors with $N = 2$ obtained with exhaustive search and with Algorithm 1.

Algorithm 1 can be implemented in a centralized manner at the BS and the covariance shaping vectors are fed back to the corresponding UEs. Alternatively, it can be implemented in a distributed fashion at the UEs. In this case, each UE can compute its covariance shaping vector without any information exchange with the other UE provided that the channel statistics of the latter are known, the order of update is fixed, and the same initial points are used.² In fact, under these conditions, the entire alternating optimization procedure can be carried out locally and independently at each UE. Note that the same considerations hold for Algorithm 2 presented in the next section.

The result of the covariance shaping optimization heavily depends on the physical scattering environment. Consider the scenario in Fig. 1(a), where there is no line-of-sight (LoS) path between the BS and the UEs, and assume that the UEs are equipped with uniform linear arrays (ULAs). In this case, as shown in Fig. 1(b), the covariance shaping vectors tend to focus their power along reflected paths that interfere with each other as little as possible while also carrying sufficient channel power, which results in a nearly interference-free transmission/reception. On the other hand, when a LoS path exists, as in the scenario in Fig. 2(a), this generally carries more channel power than any other path. In this case, as shown in Fig. 2(b), the propagation directions selected by the covariance shaping vectors tend to partially capture the LoS path while also focusing some of their power along separated reflected paths in order to achieve some degree

²Note that $\mathbf{v}_k^{(0)}$ and $\mathbf{v}_j^{(0)}$ can be any predefined pair of normalized vectors provided by the BS.

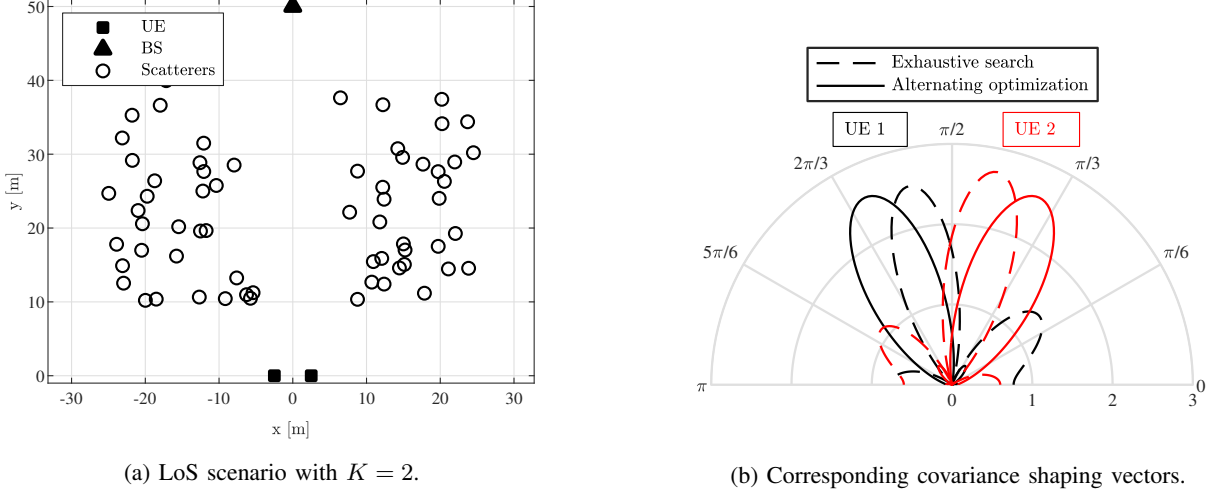


Fig. 2: (a) Map of the considered LoS scenario with $K = 2$; (b) Corresponding covariance shaping vectors with $N = 2$ obtained with exhaustive search and with Algorithm 1.

of statistical orthogonality. Remarkably, in both Fig. 1(b) and Fig. 2(b), the result of Algorithm 1 is very close to the optimal solution of problem (P1) obtained with exhaustive search over a set of 10^3 uniformly distributed vectors over the unit sphere for each UE, where the former is characterized by negligible complexity with respect to the latter.

Kronecker Channel Model. Let us consider the particular case where each channel \mathbf{H}_k is modeled using the Kronecker channel model [35]. In this setting, we have $\mathbf{H}_k = \mathbf{R}_k^{\frac{1}{2}} \mathbf{H}_k^{(w)} \mathbf{T}_k^{\frac{1}{2}}$, with \mathbf{R}_k and \mathbf{T}_k defined in Section II and $\text{vec}(\mathbf{H}_k^{(w)}) \sim \mathcal{CN}(\mathbf{0}, \mathbf{I}_{NM})$. Accordingly, the covariance matrix in (1) can be expressed as $\mathbf{\Sigma}_k = \mathbf{T}_k^T \otimes \mathbf{R}_k$ with block elements given by $\Sigma_{k,mn} = T_{k,mn}^* \mathbf{R}_k$, where $T_{k,mn}$ denotes the (m, n) th element of \mathbf{T}_k . Hence, from (26), we have

$$\delta(\mathbf{v}_k, \mathbf{v}_j) = \frac{\text{tr}((\mathbf{v}_k^H \mathbf{\Sigma}_{k,mn} \mathbf{v}_k)_{m,n=1}^M (\mathbf{v}_j^H \mathbf{\Sigma}_{j,mn}^H \mathbf{v}_j)_{m,n=1}^M)}{\text{tr}((\mathbf{v}_k^H \mathbf{\Sigma}_{k,mn} \mathbf{v}_k)_{m,n=1}^M) \text{tr}((\mathbf{v}_j^H \mathbf{\Sigma}_{j,mn}^H \mathbf{v}_j)_{m,n=1}^M)} \quad (33)$$

$$= \frac{\text{tr}((T_{k,mn} \mathbf{v}_k^H \mathbf{R}_k \mathbf{v}_k)_{m,n=1}^M (T_{j,mn} \mathbf{v}_j^H \mathbf{R}_j \mathbf{v}_j)_{m,n=1}^M)}{\text{tr}((T_{k,mn} \mathbf{v}_k^H \mathbf{R}_k \mathbf{v}_k)_{m,n=1}^M) \text{tr}((T_{j,mn} \mathbf{v}_j^H \mathbf{R}_j \mathbf{v}_j)_{m,n=1}^M)} \quad (34)$$

$$= \frac{\text{tr}(\mathbf{T}_k \mathbf{T}_j)}{\text{tr}(\mathbf{T}_k) \text{tr}(\mathbf{T}_j)}. \quad (35)$$

It is straightforward to observe that, in this case, $\delta(\mathbf{v}_k, \mathbf{v}_j)$ is independent of \mathbf{v}_k and \mathbf{v}_j . Hence, under the Kronecker channel model, it is not possible to alter the channel statistics perceived at one end of the communication link by designing the transceiver at the other end: as a consequence, no meaningful effective channel separation can be performed. This is in accordance

with the properties of the Kronecker channel model, whereby the transmit and receive covariance matrices are independent. In this context, the signal subspace separation is exclusively determined by the scattering environment and can only be achieved when $\text{tr}(\mathbf{T}_k \mathbf{T}_j) = 0$, which is rarely satisfied in practice [27], [35].

B. Multi-UE Case

In the general case, i.e., for $K \geq 2$, the covariance shaping vectors for each UE are computed by solving the optimization problem

$$\begin{aligned} & \underset{\{\mathbf{v}_k\}_{k=1}^K}{\text{minimize}} && \sum_{k \neq j} \delta(\mathbf{v}_k, \mathbf{v}_j) \\ & \text{subject to} && \{\|\mathbf{v}_k\|^2 = 1\}_{k=1}^K \end{aligned} \quad (\text{P2})$$

with $\delta(\mathbf{v}_k, \mathbf{v}_j)$ defined in (26). Although problem (P2) is not convex in any of the optimization variables $\{\mathbf{v}_k\}_{k=1}^K$, it can be efficiently solved via block coordinate descent, which can be interpreted as an extension of the alternating optimization approach presented in the previous section for the two-UE case. The optimal covariance shaping vector of UE k for given $\{\mathbf{v}_j\}_{j \neq k}$ is obtained as

$$\mathbf{v}_k^* = \underset{\mathbf{v}_k : \|\mathbf{v}_k\|^2=1}{\text{argmin}} \frac{\sum_{m,n=1}^M \mathbf{v}_k^H \left(\sum_{j \neq k} \eta_{j,mn}(\mathbf{v}_j) \boldsymbol{\Sigma}_{k,mm} \right) \mathbf{v}_k}{\mathbf{v}_k^H \left(\sum_{m=1}^M \boldsymbol{\Sigma}_{k,mm} \right) \mathbf{v}_k} \quad (36)$$

with $\eta_{j,mn}(\mathbf{v}_j)$ defined in (30). Like (31), (36) is in the form of generalized Rayleigh quotient and thus admits the solution

$$\mathbf{v}_k^* = \mathbf{u}_{\min} \left(\left(\sum_{m=1}^M \boldsymbol{\Sigma}_{k,mm} \right)^{-1} \left(\sum_{m,n=1}^M \sum_{j \neq k} \eta_{j,mn}(\mathbf{v}_j) \boldsymbol{\Sigma}_{k,mm} \right) \right) \quad (37)$$

and the optimal covariance shaping vectors of the other UEs j for given $\{\mathbf{v}_k\}_{k \neq j}$ are obtained in a similar way. Hence, problem (P2) is solved by optimizing the strategy of each UE given the strategies of the other UEs until a predetermined convergence criterion is satisfied. Furthermore, at each iteration n , the update $\mathbf{v}_k^{(n)} = \alpha \mathbf{v}_k^* + (1 - \alpha) \mathbf{v}_k^{(n-1)}$ can be used to limit the variation of the covariance shaping vectors between consecutive iterations, where the step size $\alpha \in (0, 1]$ must be chosen to strike the proper balance between convergence speed and accuracy (see, e.g., [10], [36]). The proposed scheme is formalized in Algorithm 2, whose convergence properties are characterized in Proposition 3.

Algorithm 2 (Covariance shaping: Block coordinate descent algorithm)

Data: $\{\mathbf{v}_k^{(0)}\}_{k=1}^K$, $\{\Sigma_k\}_{k=1}^K$, $\alpha \in (0, 1]$, and ϵ . Fix $n = 1$.

While $\sum_{k \neq j} |\delta(\mathbf{v}_k^{(n)}, \mathbf{v}_j^{(n)}) - \delta(\mathbf{v}_k^{(n-1)}, \mathbf{v}_j^{(n-1)})| / \delta(\mathbf{v}_k^{(n)}, \mathbf{v}_j^{(n)}) > \epsilon$

For $k = 1, \dots, K$

(S.1) Given $\{\mathbf{v}_j^{(n-1)}\}_{j \neq k}$, compute $\{\eta_{j,mn}(\mathbf{v}_j^{(n)})\}_{m,n=1}^M$ as in (30), $\forall j \neq k$.

(S.2) Compute \mathbf{v}_k^* as in (37).

(S.3) Update $\mathbf{v}_k^{(n)} = \alpha \mathbf{v}_k^* + (1 - \alpha) \mathbf{v}_k^{(n-1)}$.

End

End

(S.4) Fix $\{\mathbf{v}_k = \mathbf{v}_k^{(n)}\}_{k=1}^K$.

Proposition 3. *The block coordinate descent algorithm described in Algorithm 2 converges to a limit point of problem (P2).*

Proof: At each iteration n of Algorithm 1, the covariance shaping vector of UE k results from solving (31), which admits the optimal solution in (32). Hence, the sequence $\{\delta(\mathbf{v}_k^{(n)}, \mathbf{v}_j^{(n)})\}_n$ is non-increasing since

$$\delta(\mathbf{v}_k^{(n)}, \mathbf{v}_j^{(n-1)}) \leq \delta(\mathbf{v}_k^{(n-1)}, \mathbf{v}_j^{(n-1)}). \quad (38)$$

Moreover, since $\delta(\mathbf{v}_k, \mathbf{v}_j) \geq 0$, the sequence $\{\delta(\mathbf{v}_k^{(n)}, \mathbf{v}_j^{(n)})\}_n$ converges to a finite non-negative value. ■

V. NUMERICAL RESULTS AND DISCUSSION

In this section, we present numerical results to evaluate the gains achieved by the proposed covariance shaping framework. With this aim, we compare the following alternative transmission/reception schemes, where the first is based on covariance shaping and the other two are used as reference schemes.

- 1) **RZF+covariance shaping.** Each UE k applies its covariance shaping vector \mathbf{v}_k during both the uplink pilot-aided channel estimation phase and the downlink data transmission phase as discussed in Section IV. The BS obtains the MMSE estimates of the effective channels $\{\hat{\mathbf{g}}_k\}_{k=1}^K$ as in (10) based on the reception of $P < K$ orthogonal pilot vectors.

These estimates are used to compute regularized zero-forcing (RZF) precoding at the BS as [37]

$$\mathbf{W} = \frac{(\hat{\mathbf{H}}^H \hat{\mathbf{H}} + \frac{K}{\rho_{\text{BS}}} \mathbf{I}_M)^{-1} \hat{\mathbf{H}}^H}{\|(\hat{\mathbf{H}}^H \hat{\mathbf{H}} + \frac{K}{\rho_{\text{BS}}} \mathbf{I}_M)^{-1} \hat{\mathbf{H}}^H\|} \quad (39)$$

where we recall that $\hat{\mathbf{H}} = [\hat{\mathbf{g}}_1^T, \dots, \hat{\mathbf{g}}_K^T]^T$.

- 2) **Iterative MMSE+MMSE.** The BS obtains the MMSE estimates of the channel matrices $\{\hat{\mathbf{H}}_k\}_{k=1}^K$ as in (3) based on the reception of $P < K$ orthogonal pilot matrices. These estimates are used to compute MMSE precoding at the BS and MMSE combining at the UEs via the iterative algorithm proposed in [38].
- 3) **BD+MMSE.** The BS obtains the MMSE estimates of the channel matrices $\{\hat{\mathbf{H}}_k\}_{k=1}^K$ as in (3) based on the reception of $P < K$ orthogonal pilot matrices. These estimates are used to compute block diagonalization (BD) precoding at the BS as in [39], with water-filling power allocation. On the other hand, each UE k adopts MMSE combining with

$$\mathbf{V}_k = \frac{(\sum_{j=1}^K \hat{\mathbf{H}}_k \mathbf{W}_j \mathbf{W}_j^H \hat{\mathbf{H}}_k^H + \frac{1}{\rho_{\text{BS}}} \mathbf{I}_N)^{-1} \hat{\mathbf{H}}_k \mathbf{W}_k}{\|(\sum_{j=1}^K \hat{\mathbf{H}}_k \mathbf{W}_j \mathbf{W}_j^H \hat{\mathbf{H}}_k^H + \frac{1}{\rho_{\text{BS}}} \mathbf{I}_N)^{-1} \hat{\mathbf{H}}_k \mathbf{W}_k\|}. \quad (40)$$

Some comments are in order.

- The schemes in 2) and 3) imply that the UEs have the same knowledge of the estimated instantaneous channels as the BS as well as perfect knowledge of the instantaneous precoding strategy used by the BS, both of which are necessary to implement MMSE combining. Note that such information must be acquired by each UE in each coherence block via extra feedback resources. On the other hand, the proposed covariance shaping approach relies solely on statistical CSI, i.e., slowly varying information, which substantially reduces the need for extra feedback resources.
- The schemes in 2) and 3) require antenna-specific pilots for the estimation of the channel matrices $\{\mathbf{H}_k\}_{k=1}^K$. In particular, N orthogonal pilot vectors are assigned to each UE, which implies $\tau \geq PN$. On the other hand, the estimation of the effective channels $\{\bar{\mathbf{g}}_k\}_{k=1}^K$ resulting from covariance shaping requires $\tau \geq P$ and, therefore, the pilot length can be potentially reduced.
- The schemes in 2) and 3) allow the transmission of up to N streams per UE, while only one stream per UE is transmitted when covariance shaping is used. In the following, we

demonstrate how the proposed covariance shaping method can effectively outperform the reference schemes, which employ the multiple antennas at the UE for spatial multiplexing, in scenarios where the UEs exhibit high spatial correlation.

We consider a scenario in which the BS serves K closely spaced UEs. We assume that both the BS and the UEs are equipped with ULAs, and the channel between the BS and each UE k follows the discrete physical channel model in [40]. In this context, we define the linear array responses at each UE for the angle of impingement θ and at the BS for the angle of impingement ϕ as

$$\mathbf{a}(\theta) \triangleq [1, e^{-2\pi\delta \sin(\theta)}, \dots, e^{-2\pi\delta(N-1)\sin(\theta)}]^\text{T} \in \mathbb{C}^{N \times 1}, \quad (41)$$

$$\mathbf{b}(\phi) \triangleq [1, e^{-2\pi\delta \sin(\phi)}, \dots, e^{-2\pi\delta(M-1)\sin(\phi)}]^\text{T} \in \mathbb{C}^{M \times 1} \quad (42)$$

respectively, where $\delta = 0.5$ represents the ratio between the antenna spacing and the signal wavelength. Then, for each UE k , we have

$$\mathbf{H}_k = \sqrt{\frac{\kappa}{1+\kappa}} d_k^{-\frac{\beta}{2}} \mathbf{a}(\theta_k) \mathbf{b}(\phi_k)^\text{H} + \sqrt{\frac{1}{1+\kappa}} \sum_{l=1}^{L_p} d_{k,l}^{-\frac{\beta}{2}} \alpha_{k,l} \mathbf{a}(\theta_{k,l}) \mathbf{b}(\phi_{k,l})^\text{H} \quad (43)$$

where κ is the Ricean factor, L_p is the number of reflected paths, d_k and $d_{k,l}$ are the distances of the LoS path and of the l th reflected path, respectively, θ_k and $\theta_{k,l}$ are the angles of impingement at the UE of the LoS path and of the l th reflected path, respectively, ϕ_k and $\phi_{k,l}$ are the angles of impingement at the BS of the LoS path and of the l th reflected path, respectively, $\alpha_{k,l}$ is the random phase delay of the l th reflected path, and β is the pathloss exponent. Unless otherwise stated, we use the simulation parameters listed in Table I. The following results are obtained by means of Monte Carlo simulations with 5×10^3 independent channel realizations. Lastly, we point out that, for the considered scenarios, we observe that Algorithms 1 and 2 always converge in very few iterations, i.e., less than 10.

A. Two-UE case

With reference to Section IV-A, we first examine the simple case of $K = 2$ UEs with $N = 2$ antennas each in order to highlight the key characteristics of the proposed covariance shaping framework. In this setting, we assume $P = 1$, i.e., the UEs are assigned the same pilot, and we remark that there is no pilot contamination among the antennas of a given UE for the schemes in 2) and 3). We consider the LoS and NLoS scenarios illustrated in Fig. 1(a) and in Fig. 2(a),

Parameter	Symbol	Value
Number of BS antennas	M	128
Number of UEs	K	$\{2, 4\}$
Number of UE antennas	N	$\{2, 3\}$
Noise variance at the BS	σ_{BS}^2	-80 dBm
Noise variance at the UEs	σ_{UE}^2	-80 dBm
Transmit power at the BS	ρ_{BS}	30 dBm
Transmit power at the UEs	ρ_{UE}	25 dBm
Number of orthogonal pilots	P	$\lceil \frac{K}{2} \rceil$
Pilot length	τ	16
Ricean factor	κ	2.5 (LoS), 0 (NLoS)
Pathloss exponent	β	2

TABLE I: Simulation parameters.

respectively, and the corresponding covariance shaping vectors are shown in Fig. 1(b) and in Fig. 2(b), respectively. Observe that, in this case, the distance between the UEs is 4 m, which is small compared with the distance of about 50 m between the UEs and the BS and results in highly overlapping covariance matrices.

Let us define the normalized MSE (NMSE) of the channel estimation for UE k as

$$\overline{\text{NMSE}}_k \triangleq \mathbb{E} \left[\frac{\|\hat{\mathbf{g}}_k - \bar{\mathbf{g}}_k\|^2}{\|\bar{\mathbf{g}}_k\|^2} \right] \quad (44)$$

for the effective channels $\{\hat{\mathbf{g}}_k\}_{k=1}^K$ resulting from covariance shaping and

$$\text{NMSE}_k \triangleq \frac{1}{N} \sum_{n=1}^N \mathbb{E} \left[\frac{\|\hat{\mathbf{g}}_{k,n} - \mathbf{g}_{k,n}\|^2}{\|\mathbf{g}_{k,n}\|^2} \right] \quad (45)$$

for the channel matrices $\{\hat{\mathbf{H}}_k\}_{k=1}^K$. Considering the NLoS scenario, Fig. 3 plots the NMSE of the channel estimation versus the transmit power at the UEs. We observe that, thanks to the improved statistical orthogonality, the proposed covariance shaping method considerably increases the channel estimation accuracy with respect to the reference schemes, which are severely limited by pilot contamination. Fig. 4 plots the average sum rate against the transmit power at the BS. Here, it is straightforward to see that the signal subspace separation enforced by covariance shaping during both the uplink pilot-aided channel estimation phase and the downlink data transmission phase has a highly beneficial effect on the system performance.

To quantify the degree of orthogonality between the covariance matrices of the two UEs, we

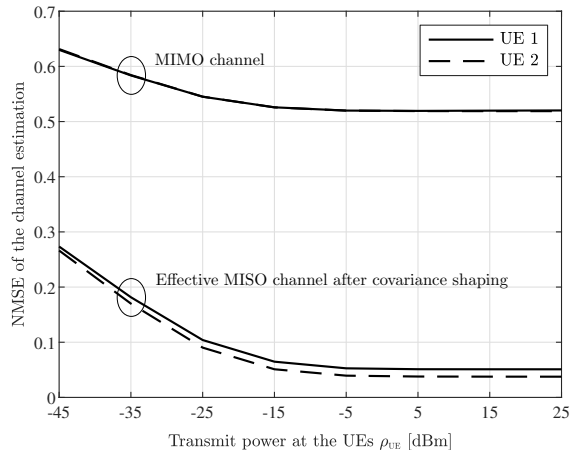


Fig. 3: NMSE of the channel estimation versus transmit power at the UEs for the NLoS scenario depicted in Fig. 1(a), with $K = 2$ and $N = 2$.

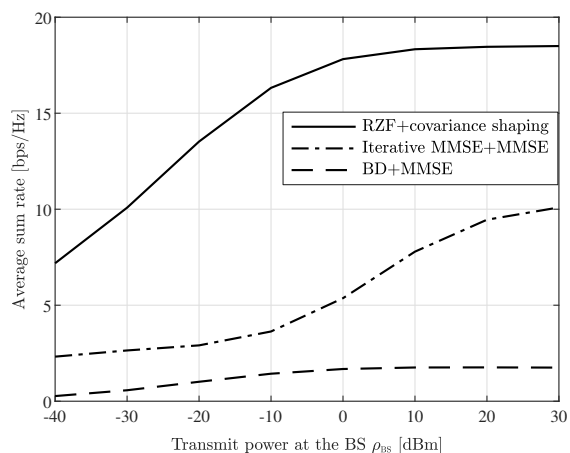


Fig. 4: Average sum rate versus transmit power at the BS for the NLoS scenario depicted in Fig. 1(a), with $K = 2$ and $N = 2$.

use the notion of *chordal distance* [20], defined as

$$d_c \triangleq \|\mathbf{U}_k \mathbf{U}_k^H - \mathbf{U}_j \mathbf{U}_j^H\|_F^2 \quad (46)$$

where $\mathbf{U}_k \in \mathbb{C}^{NM \times NM}$ contains the eigenvectors of $\mathbf{\Sigma}_k$ in (1), i.e., the covariance matrix of UE k . Considering the LoS scenario, Fig. 5 plots the average sum rate against the chordal distance between the covariance matrices of the two UEs as they move away from each other. Here, $d_c = 0$ corresponds to the case where the two UEs are co-located and thus have identical covariance matrices, whereas $d_c = 15$ corresponds to the case where the two UEs are 5 m apart. Evidently, the reference schemes are markedly limited by the overlapping covariance matrices of the UEs, which yields a generally poor performance. On the other hand, the proposed covariance

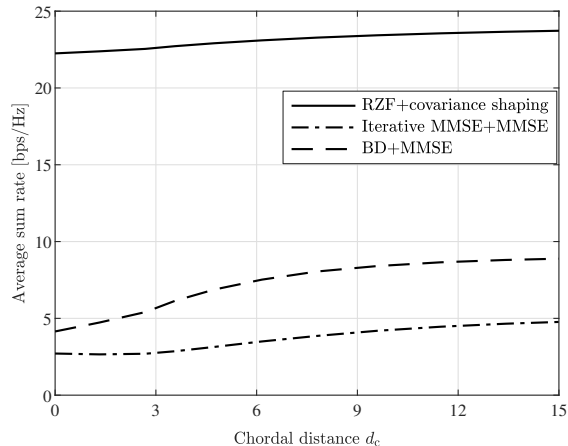


Fig. 5: Average sum rate versus chordal distance for the LoS scenario depicted in Fig. 2(a), with $K = 2$ and $N = 2$.

shaping approach is able to enforce statistical orthogonality even when the UEs are closely spaced.

B. Multi-UE Case

With reference to Section IV-B, we now examine the case of $K = 4$ UEs with $N = 3$ antennas each and consider the NLoS scenarios illustrated in Fig. 6(a). The distance between adjacent UEs is 3 m, which results in highly overlapping covariance matrices. In this setting, $P = 2$ orthogonal pilots are assigned such that two adjacent UEs always utilize orthogonal pilots. The covariance shaping vectors obtained with Algorithm 2 are shown in Fig. 6(b), which tend to focus their power along reflected paths that are as orthogonal as possible to each other while also carrying sufficient channel power (cf. Fig. 1(b)).

Fig. 7 plots the average sum rate against the transmit power at the BS. As in Fig. 4, the reference schemes are hindered by the spatial correlation among the UEs despite the availability of multiple degrees of freedom at the latter, which allows to transmit multiple streams per UE. On the other hand, the proposed covariance shaping method achieves remarkable performance gains in terms of average sum rate by transmitting only one stream per UE in the directions dictated by the covariance shaping vectors. Fig. 8 plots the average sum rate against the number of BS antennas, showing the benefits of increasing the array size for all the considered schemes. In particular, we observe that increasing the spatial resolution at the BS does not fundamentally solve the limitations of the reference scenarios when the UEs exhibit high spatial correlation.

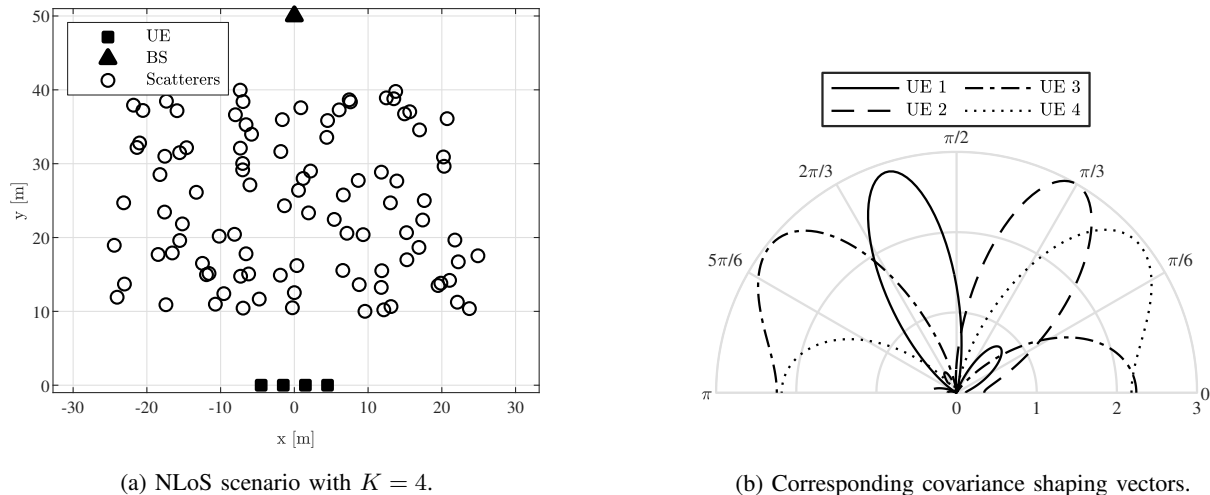


Fig. 6: (a) Map of the considered NLoS scenario with $K = 4$; (b) Corresponding covariance shaping vectors with $N = 3$ obtained with Algorithm 2.

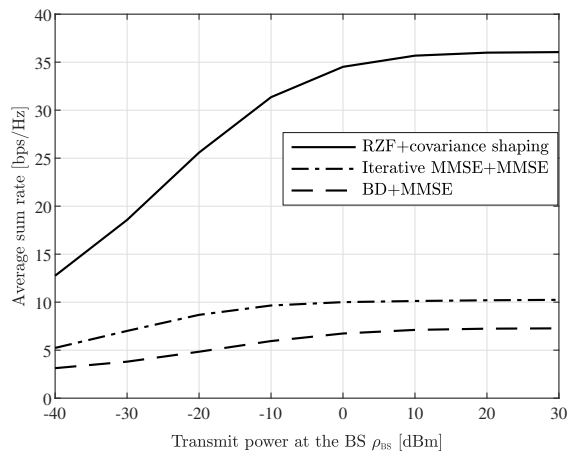


Fig. 7: Average sum rate versus transmit power at the BS for the NLoS scenario depicted in Fig. 6(a), with $K = 4$ and $N = 3$.

Lastly, Fig. 9 plots the average sum rate versus the number of UEs, where $P = \lceil \frac{K}{2} \rceil$ orthogonal pilots are assigned such that two adjacent UEs always utilize orthogonal pilots. Here, the single-UE case, i.e., $K = 1$, is included to illustrate that the reference schemes outperform the proposed covariance shaping method when multiple antennas at the UE can be effectively used for spatial multiplexing. On the other hand, for $K \geq 2$, covariance shaping guarantees significant performance gains by enforcing signal subspace separation among the UEs.

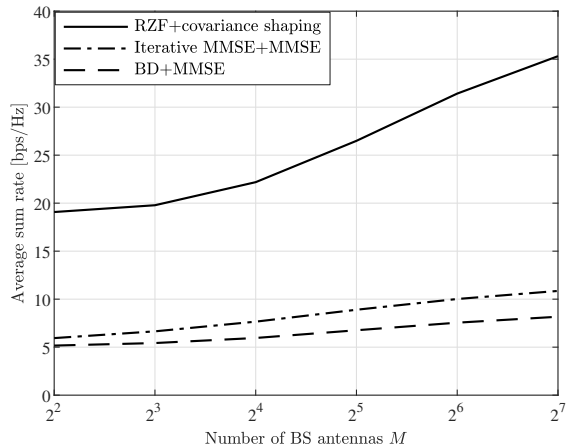


Fig. 8: Average sum rate versus the number of BS antennas for the NLoS scenario depicted in Fig. 6(a), with $K = 4$ and $N = 3$.

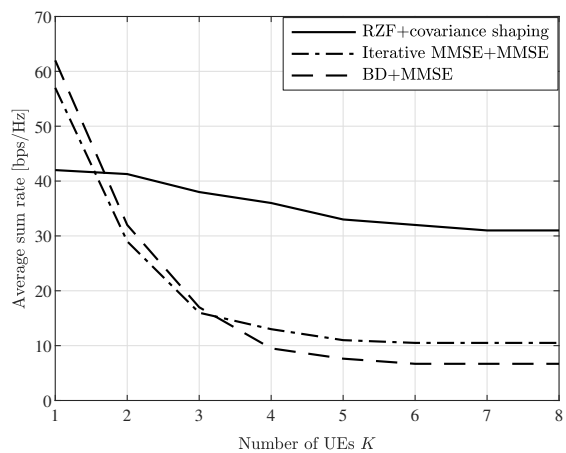


Fig. 9: Average sum rate versus number of UEs for the NLoS scenario depicted in Fig. 6(a), with $N = 3$.

VI. CONCLUSIONS

In this paper, we introduce the novel concept of MIMO covariance shaping as a means to achieve statistical orthogonality among interfering UEs. It consists in preemptively applying a statistical beamforming at each UE during both the uplink pilot-aided channel estimation phase and the downlink data transmission phase, aiming at enforcing a separation of the signal subspaces of the UEs that would be otherwise highly overlapping. The proposed MIMO covariance shaping framework exploits the realistic non-Kronecker structure of massive MIMO channels, which allows to suitably alter the channel statistics perceived at the BS by proper design of the transceiver at the UE-side. To compute the covariance shaping strategies, we present a low-complexity block coordinate descent algorithm that minimizes the inter-UE interference (as a

metric to measure the spatial correlation) and is proved to converge to a limit point of the original nonconvex problem or to a stationary point in the two-UE case. This results in a superior sum-rate performance with respect to reference schemes employing the multiple antennas at the UE for spatial multiplexing in scenarios where the UEs have highly overlapping covariance matrices and the channel estimation is limited by strong pilot contamination. Future work will consider MIMO covariance shaping in combination with multi-stream transmission and will analyze the tradeoff between statistical orthogonality and spatial multiplexing.

APPENDIX I

DERIVATIONS OF THE EFFECTIVE SINR IN (19)

Given the multi-UE effective channel matrix $\bar{\mathbf{H}} = [\bar{\mathbf{g}}_1^T, \dots, \bar{\mathbf{g}}_K^T]^T \in \mathbb{C}^{K \times M}$, where the effective channels $\{\bar{\mathbf{g}}_k\}_{k=1}^K$ are mutually independent, we have

$$\mathbb{E}[\|\bar{\mathbf{H}}\|_{\text{F}}^2] = \mathbb{E}[\text{tr}(\bar{\mathbf{H}}\bar{\mathbf{H}}^H)] \quad (47)$$

$$= \text{tr}(\mathbb{E}[\bar{\mathbf{H}}\bar{\mathbf{H}}^H]) \quad (48)$$

$$= \sum_{k=1}^K \text{tr}(\bar{\Phi}_k) \quad (49)$$

where we recall that $\bar{\mathbf{g}}_k \sim \mathcal{CN}(\mathbf{0}, \bar{\Phi}_k)$.

Considering now a random vector $\mathbf{x} \in \mathbb{C}^{M \times 1}$ and a Hermitian matrix $\mathbf{A} \in \mathbb{C}^{M \times M}$, we have

$$\mathbb{E}[\mathbf{x}\mathbf{x}^H \mathbf{A} \mathbf{x}\mathbf{x}^H] = \left(\mathbb{E} \left[\sum_{u=1}^M \sum_{v=1}^M A_{uv} x_s^* x_t x_u^* x_v \right] \right)_{s,t=1}^M \quad (50)$$

where A_{uv} is the (u, v) th element of \mathbf{A} and x_s is the s th element of \mathbf{x} , with

$$\mathbb{E} \left[A_{uv} x_s^* x_t x_u^* x_v \right] = \begin{cases} \mu_4 A_{uu}, & \text{if } s = t = u = v \\ \mu_2^2 A_{uu}, & \text{if } s = t \neq u = v \\ \mu_2^2 A_{uv}, & \text{if } s = u \neq t = v \\ 0, & \text{otherwise} \end{cases} \quad (51)$$

where μ_2 and μ_4 are the second- and fourth-order moments of \mathbf{x} , respectively. When $\mathbf{x} \sim$

$\mathcal{CN}(\mathbf{0}, \mathbf{I}_M)$, we have $\mu_2 = 1$ and $\mu_4 = 2$, and we obtain

$$\mathbb{E} \left[\sum_{u=1}^M \sum_{v=1}^M A_{uv} x_s^* x_t x_u^* x_v \right] = \begin{cases} 2A_{tt} + (\text{tr}(\mathbf{A}) - A_{tt}), & \text{if } s = t \\ A_{st}, & \text{if } s \neq t \end{cases} \quad (52)$$

which yields

$$\mathbb{E}[\mathbf{x}\mathbf{x}^H \mathbf{A} \mathbf{x}\mathbf{x}^H] = \mathbf{A} + \text{tr}(\mathbf{A})\mathbf{I}_M. \quad (53)$$

Let us define $\mathbf{n} \triangleq \mathbf{Z}\mathbf{p}^H \in \mathbb{C}^{M \times 1}$, which is distributed as $\mathcal{CN}(\mathbf{0}, \sigma_{\text{BS}}^2 \mathbf{I}_M)$. Hence, the variance of $\bar{\mathbf{g}}_k \hat{\mathbf{g}}_k^H$ can be expressed as

$$\mathbb{V}[\bar{\mathbf{g}}_k \hat{\mathbf{g}}_k^H] = \mathbb{E}[|\bar{\mathbf{g}}_k \hat{\mathbf{g}}_k^H|^2] - |\mathbb{E}[\bar{\mathbf{g}}_k \hat{\mathbf{g}}_k^H]|^2 \quad (54)$$

$$\begin{aligned} &= \mathbb{E} \left[\left(\bar{\mathbf{g}}_k \bar{\Phi}_k \mathbf{Q}_k^{-1} \left(\bar{\mathbf{g}}_k^H + \sum_{j \in \mathcal{S}_p \setminus \{k\}} \bar{\mathbf{g}}_j^H + \frac{1}{\sqrt{\rho_{\text{UE}}}} \mathbf{n} \right) \right) \right. \\ &\quad \times \left. \left(\left(\bar{\mathbf{g}}_k + \sum_{j \in \mathcal{S}_p \setminus \{k\}} \bar{\mathbf{g}}_j + \frac{1}{\sqrt{\rho_{\text{UE}}}} \mathbf{n}^H \right) \mathbf{Q}_k^{-1} \bar{\Phi}_k \bar{\mathbf{g}}_k^H \right) \right] \\ &\quad - \left| \mathbb{E} \left[\bar{\mathbf{g}}_k \bar{\Phi}_k \mathbf{Q}_k^{-1} \left(\bar{\mathbf{g}}_k^H + \sum_{j \in \mathcal{S}_p \setminus \{k\}} \bar{\mathbf{g}}_j^H + \frac{1}{\sqrt{\rho_{\text{UE}}}} \mathbf{n} \right) \right] \right|^2 \end{aligned} \quad (55)$$

$$\begin{aligned} &= \mathbb{E}[\bar{\mathbf{g}}_k \bar{\Phi}_k \mathbf{Q}_k^{-1} \bar{\mathbf{g}}_k^H \bar{\mathbf{g}}_k \mathbf{Q}_k^{-1} \bar{\Phi}_k \bar{\mathbf{g}}_k^H] + \sum_{j \in \mathcal{S}_p \setminus \{k\}} \mathbb{E}[\bar{\mathbf{g}}_k \bar{\Phi}_k \mathbf{Q}_k^{-1} \bar{\mathbf{g}}_j^H \bar{\mathbf{g}}_j \mathbf{Q}_k^{-1} \bar{\Phi}_k \bar{\mathbf{g}}_k^H] \\ &\quad + \frac{1}{\rho_{\text{UE}}} \mathbb{E}[\bar{\mathbf{g}}_k \bar{\Phi}_k \mathbf{Q}_k^{-1} \mathbf{n} \mathbf{n}^H \mathbf{Q}_k^{-1} \bar{\Phi}_k \bar{\mathbf{g}}_k^H] - |\mathbb{E}[\bar{\mathbf{g}}_k \bar{\Phi}_k \mathbf{Q}_k^{-1} \bar{\mathbf{g}}_k^H]|^2 \end{aligned} \quad (56)$$

where in (55) we have used the expression of $\hat{\mathbf{g}}_k$ in (10) and in (56) we have exploited the independence between $\bar{\mathbf{g}}_k$ and $\bar{\mathbf{g}}_j$, $\forall k \neq j$, and between $\bar{\mathbf{g}}_k$ and \mathbf{n} . Since each $\bar{\mathbf{g}}_k$ can be expressed as $\bar{\mathbf{g}}_k = \bar{\mathbf{g}}_k^{(0)} \bar{\Phi}_k^{\frac{1}{2}}$, where $\bar{\mathbf{g}}_k^{(0)} \in \mathbb{C}^{1 \times M}$ is distributed as $\sim \mathcal{CN}(0, \mathbf{I}_M)$, we have

$$\begin{aligned} \mathbb{V}[\bar{\mathbf{g}}_k \hat{\mathbf{g}}_k^H] &= \mathbb{E}[\bar{\mathbf{g}}_k^{(0)} \bar{\Phi}_k^{\frac{1}{2}} \bar{\Phi}_k \mathbf{Q}_k^{-1} \bar{\Phi}_k^{\frac{1}{2}} (\bar{\mathbf{g}}_k^{(0)})^H \bar{\mathbf{g}}_k^{(0)} \bar{\Phi}_k^{\frac{1}{2}} \mathbf{Q}_k^{-1} \bar{\Phi}_k \bar{\Phi}_k^{\frac{1}{2}} (\bar{\mathbf{g}}_k^{(0)})^H] \\ &\quad + \sum_{j \in \mathcal{S}_p \setminus \{k\}} \mathbb{E}[\bar{\mathbf{g}}_k^{(0)} \bar{\Phi}_k^{\frac{1}{2}} \bar{\Phi}_k \mathbf{Q}_k^{-1} \bar{\Phi}_k^{\frac{1}{2}} (\bar{\mathbf{g}}_j^{(0)})^H \bar{\mathbf{g}}_j^{(0)} \bar{\Phi}_j^{\frac{1}{2}} \mathbf{Q}_k^{-1} \bar{\Phi}_k \bar{\Phi}_k^{\frac{1}{2}} (\bar{\mathbf{g}}_k^{(0)})^H] \\ &\quad + \frac{1}{\rho_{\text{UE}}} \mathbb{E}[\bar{\mathbf{g}}_k^{(0)} \bar{\Phi}_k^{\frac{1}{2}} \bar{\Phi}_k \mathbf{Q}_k^{-1} \mathbf{n} \mathbf{n}^H \mathbf{Q}_k^{-1} \bar{\Phi}_k \bar{\Phi}_k^{\frac{1}{2}} (\bar{\mathbf{g}}_k^{(0)})^H] - |\mathbb{E}[\bar{\mathbf{g}}_k^{(0)} \bar{\Phi}_k^{\frac{1}{2}} \bar{\Phi}_k \mathbf{Q}_k^{-1} \bar{\Phi}_k^{\frac{1}{2}} (\bar{\mathbf{g}}_k^{(0)})^H]|^2. \end{aligned} \quad (57)$$

Rearranging the terms, we obtain

$$\begin{aligned}
\mathbb{V}[\bar{\mathbf{g}}_k \hat{\mathbf{g}}_k^H] &= \text{tr} \left(\bar{\Phi}_k^{\frac{1}{2}} \bar{\Phi}_k \mathbf{Q}_k^{-1} \bar{\Phi}_k^{\frac{1}{2}} \mathbb{E} \left[(\bar{\mathbf{g}}_k^{(0)})^H \bar{\mathbf{g}}_k^{(0)} \bar{\Phi}_k^{\frac{1}{2}} \mathbf{Q}_k^{-1} \bar{\Phi}_k \bar{\Phi}_k^{\frac{1}{2}} (\bar{\mathbf{g}}_k^{(0)})^H \bar{\mathbf{g}}_k^{(0)} \right] \right) \\
&+ \sum_{j \in \mathcal{S}_p \setminus \{k\}} \text{tr} \left(\mathbb{E} \left[(\bar{\mathbf{g}}_k^{(0)})^H \bar{\mathbf{g}}_k^{(0)} \right] \bar{\Phi}_k^{\frac{1}{2}} \bar{\Phi}_k \mathbf{Q}_k^{-1} \bar{\Phi}_j^{\frac{1}{2}} \mathbb{E} \left[(\bar{\mathbf{g}}_j^{(0)})^H \bar{\mathbf{g}}_j^{(0)} \right] \bar{\Phi}_j^{\frac{1}{2}} \mathbf{Q}_k^{-1} \bar{\Phi}_k \bar{\Phi}_k^{\frac{1}{2}} \right) \\
&+ \frac{1}{\rho_{\text{UE}}} \text{tr} \left(\mathbb{E} \left[(\bar{\mathbf{g}}_k^{(0)})^H \bar{\mathbf{g}}_k^{(0)} \right] \bar{\Phi}_k^{\frac{1}{2}} \bar{\Phi}_k \mathbf{Q}_k^{-1} \mathbb{E}[\mathbf{nn}^H] \mathbf{Q}_k^{-1} \bar{\Phi}_k \bar{\Phi}_k^{\frac{1}{2}} \right) \\
&- \text{tr} \left(\mathbb{E} \left[(\bar{\mathbf{g}}_k^{(0)})^H \bar{\mathbf{g}}_k^{(0)} \right] \bar{\Phi}_k^{\frac{1}{2}} \bar{\Phi}_k \mathbf{Q}_k^{-1} \bar{\Phi}_k^{\frac{1}{2}} \right)^2 \tag{58}
\end{aligned}$$

$$\begin{aligned}
&= \text{tr}(\bar{\Phi}_k^2 \mathbf{Q}_k^{-1} \bar{\Phi}_k \mathbf{Q}_k^{-1} \bar{\Phi}_k) + \text{tr}(\bar{\Phi}_k \mathbf{Q}_k^{-1} \bar{\Phi}_k)^2 + \sum_{j \in \mathcal{S}_p \setminus \{k\}} \text{tr}(\bar{\Phi}_k^2 \mathbf{Q}_k^{-1} \bar{\Phi}_j \mathbf{Q}_k^{-1} \bar{\Phi}_k) \\
&+ \frac{1}{\rho_{\text{UE}}} \text{tr}(\bar{\Phi}_k^2 \mathbf{Q}_k^{-2} \bar{\Phi}_k) - \text{tr}(\bar{\Phi}_k \mathbf{Q}_k^{-1} \bar{\Phi}_k)^2 \tag{59}
\end{aligned}$$

$$= \text{tr}(\bar{\Phi}_k^2 \mathbf{Q}_k^{-1} \bar{\Phi}_k \mathbf{Q}_k^{-1} \bar{\Phi}_k) + \sum_{j \in \mathcal{S}_p \setminus \{k\}} \text{tr}(\bar{\Phi}_k^2 \mathbf{Q}_k^{-1} \bar{\Phi}_j \mathbf{Q}_k^{-1} \bar{\Phi}_k) + \frac{1}{\rho_{\text{UE}}} \text{tr}(\bar{\Phi}_k^2 \mathbf{Q}_k^{-2} \bar{\Phi}_k) \tag{60}$$

$$= \text{tr} \left(\bar{\Phi}_k^2 \mathbf{Q}_k^{-1} \left(\bar{\Phi}_k + \sum_{j \in \mathcal{S}_p \setminus \{k\}} \bar{\Phi}_j + \frac{1}{\rho_{\text{UE}}} \mathbf{I}_M \right) \mathbf{Q}_k^{-1} \bar{\Phi}_k \right) \tag{61}$$

$$= \text{tr}(\bar{\Phi}_k^2 \mathbf{Q}_k^{-1} \bar{\Phi}_k) \tag{62}$$

where in (59) we have used the property in (53). Finally, following similar steps, the expectation of $|\bar{\mathbf{g}}_k \hat{\mathbf{g}}_j^H|^2$ can be expressed as

$$\begin{aligned}
\mathbb{E}[|\bar{\mathbf{g}}_k \hat{\mathbf{g}}_j^H|^2] &= \sum_{\ell \in \mathcal{S}_p \setminus \{j\}} \text{tr} \left(\mathbb{E} \left[(\bar{\mathbf{g}}_k^{(0)})^H \bar{\mathbf{g}}_k^{(0)} \right] \bar{\Phi}_k^{\frac{1}{2}} \bar{\Phi}_j \mathbf{Q}_j^{-1} \bar{\Phi}_\ell^{\frac{1}{2}} \mathbb{E} \left[(\bar{\mathbf{g}}_\ell^{(0)})^H \bar{\mathbf{g}}_\ell^{(0)} \right] \bar{\Phi}_\ell^{\frac{1}{2}} \mathbf{Q}_j^{-1} \bar{\Phi}_j \bar{\Phi}_k^{\frac{1}{2}} \right) \\
&+ \text{tr} \left(\mathbb{E} \left[(\bar{\mathbf{g}}_k^{(0)})^H \bar{\mathbf{g}}_k^{(0)} \right] \bar{\Phi}_k^{\frac{1}{2}} \bar{\Phi}_j \mathbf{Q}_j^{-1} \bar{\Phi}_j^{\frac{1}{2}} \mathbb{E} \left[(\bar{\mathbf{g}}_j^{(0)})^H \bar{\mathbf{g}}_j^{(0)} \right] \bar{\Phi}_j^{\frac{1}{2}} \mathbf{Q}_j^{-1} \bar{\Phi}_j \bar{\Phi}_k^{\frac{1}{2}} \right) \\
&+ \frac{1}{\rho_{\text{UE}}} \text{tr} \left(\mathbb{E} \left[(\bar{\mathbf{g}}_k^{(0)})^H \bar{\mathbf{g}}_k^{(0)} \right] \bar{\Phi}_k^{\frac{1}{2}} \bar{\Phi}_j \mathbf{Q}_j^{-1} \mathbb{E}[\mathbf{nn}^H] \mathbf{Q}_j^{-1} \bar{\Phi}_j \bar{\Phi}_k^{\frac{1}{2}} \right) \tag{63}
\end{aligned}$$

$$\begin{aligned}
&= \sum_{\ell \in \mathcal{S}_p \setminus \{j\}} \text{tr}(\bar{\Phi}_k \bar{\Phi}_j \mathbf{Q}_j^{-1} \bar{\Phi}_\ell \mathbf{Q}_j^{-1} \bar{\Phi}_j) + \mathbb{1}_{\mathcal{S}_p}(k, j) \text{tr}(\bar{\Phi}_k \mathbf{Q}_j^{-1} \bar{\Phi}_j)^2 \\
&+ \text{tr}(\bar{\Phi}_k \bar{\Phi}_j \mathbf{Q}_j^{-1} \bar{\Phi}_j \mathbf{Q}_j^{-1} \bar{\Phi}_j) + \frac{1}{\rho_{\text{UE}}} \text{tr}(\bar{\Phi}_k \bar{\Phi}_j \mathbf{Q}_j^{-2} \bar{\Phi}_j) \tag{64}
\end{aligned}$$

$$= \text{tr} \left(\bar{\Phi}_k \bar{\Phi}_j \mathbf{Q}_j^{-1} \left(\bar{\Phi}_j + \sum_{\ell \in \mathcal{S}_p \setminus \{j\}} \bar{\Phi}_\ell + \frac{1}{\rho_{\text{UE}}} \mathbf{I}_M \right) \mathbf{Q}_j^{-1} \bar{\Phi}_j \right) + \mathbb{1}_{\mathcal{S}_p}(k, j) \text{tr}(\bar{\Phi}_k \mathbf{Q}_j^{-1} \bar{\Phi}_j)^2 \tag{65}$$

$$= \text{tr}(\bar{\Phi}_k \bar{\Phi}_j \mathbf{Q}_j^{-1} \bar{\Phi}_j) + \mathbb{1}_{\mathcal{S}_p}(k, j) \text{tr}(\bar{\Phi}_k \mathbf{Q}_j^{-1} \bar{\Phi}_j)^2. \tag{66}$$

REFERENCES

- [1] P. Mursia, I. Atzeni, D. Gesbert, and L. Cottatellucci, "Covariance shaping for massive MIMO systems," in *Proc. IEEE Global Commun. Conf. (GLOBECOM)*, Abu Dhabi, UAE, Dec. 2018.
- [2] ———, "On the performance of covariance shaping in massive MIMO systems," in *Proc. IEEE Int. Workshop Computer-Aided Modeling and Design of Commun. Links and Netw. (CAMAD)*, Barcelona, Spain, Sep. 2018.
- [3] F. Boccardi, R. W. Heath, A. Lozano, T. L. Marzetta, and P. Popovski, "Five disruptive technology directions for 5G," *IEEE Commun. Mag.*, vol. 52, no. 2, pp. 74–80, Feb. 2014.
- [4] E. Larsson, O. Edfors, F. Tufvesson, and T. L. Marzetta, "Massive MIMO for next generation wireless systems," *IEEE Commun. Mag.*, vol. 52, no. 2, pp. 186–195, Feb. 2014.
- [5] J. G. Andrews, S. Buzzi, W. Choi, S. V. Hanly, A. Lozano, A. C. K. Soong, and J. C. Zhang, "What will 5G be?" *IEEE J. Sel. Areas Commun.*, vol. 32, no. 6, pp. 1065–1082, Jun. 2014.
- [6] N. Rajatheva, I. Atzeni, E. Björnson *et al.*, "White paper on broadband connectivity in 6G," Jun. 2020. [Online]. Available: <http://jultika.oulu.fi/files/isbn9789526226798.pdf>
- [7] J. Zhang, E. Björnson, M. Matthaiou, D. Wing, K. Ng, H. Yang, and D. J. Love, "Prospective multiple antenna technologies for beyond 5G," *IEEE J. Sel. Areas Commun.*, vol. 38, no. 8, pp. 1637–1660, Aug. 2020.
- [8] X. Chen, D. W. K. Ng, W. Yu, E. G. Larsson, N. Al-Dhahir, and R. Schober, "Massive access for 5G and beyond," *IEEE J. Sel. Areas Commun.*, vol. 39, no. 3, pp. 615–637, Mar. 2021.
- [9] H. Q. Ngo, A. Ashikhmin, H. Yang, E. G. Larsson, and T. L. Marzetta, "Cell-free massive MIMO versus small cells," *IEEE Trans. Wireless Commun.*, vol. 16, no. 3, pp. 1834–1850, Mar. 2017.
- [10] I. Atzeni, B. Gouda, and A. Tölili, "Distributed precoding design via over-the-air signaling for cell-free massive MIMO," *IEEE Trans. Wireless Commun.*, vol. 20, no. 2, pp. 1201–1216, Feb. 2021.
- [11] J. Nam, J. Y. Ahn, A. Adhikary, and G. Caire, "Joint spatial division and multiplexing: Realizing massive MIMO gains with limited channel state information," in *Proc. Conf. on Inf. Sci. and Sys. (CISS)*, Princeton, USA, Mar. 2012.
- [12] J. Jose, A. Ashikhmin, T. L. Marzetta, and S. Vishwanath, "Pilot contamination and precoding in multi-cell TDD systems," *IEEE Trans. Wireless Commun.*, vol. 10, no. 8, pp. 2640–2651, Aug. 2011.
- [13] T. L. Marzetta, E. G. Larsson, and H. Yang, *Fundamentals of Massive MIMO*. Cambridge University Press, 2016.
- [14] E. Björnson, J. Hoydis, and L. Sanguinetti, "Massive MIMO has unlimited capacity," *IEEE Trans. Wireless Commun.*, vol. 17, no. 1, pp. 574–590, Jan. 2018.
- [15] H. Yin, D. Gesbert, M. Filippou, and Y. Liu, "A coordinated approach to channel estimation in large-scale multiple-antenna systems," *IEEE J. Sel. Areas Commun.*, vol. 31, no. 2, pp. 264–273, Feb. 2013.
- [16] H. Yin, D. Gesbert, and L. Cottatellucci, "Dealing with interference in distributed large-scale MIMO systems: A statistical approach," *IEEE J. Sel. Topics Signal Process.*, vol. 8, no. 5, pp. 942–953, Oct. 2014.
- [17] X. Zhang, D. P. Palomar, and B. Ottersten, "Statistically robust design of linear MIMO transceivers," *IEEE Trans. Signal Process.*, vol. 56, no. 8, pp. 3678–3689, Aug. 2008.
- [18] M. Dai and B. Clerckx, "Transmit beamforming for MISO broadcast channels with statistical and delayed CSIT," *IEEE Trans. Commun.*, vol. 63, no. 4, pp. 1202–1215, Jan. 2015.
- [19] A. Adhikary, J. Nam, J. Y. Ahn, and G. Caire, "Joint spatial division and multiplexing—The large-scale array regime," *IEEE Trans. Inf. Theory*, vol. 59, no. 10, pp. 6441–6463, Jun. 2013.
- [20] J. Nam, A. Adhikary, J. Y. Ahn, and G. Caire, "Joint spatial division and multiplexing: Opportunistic beamforming, user grouping and simplified downlink scheduling," *IEEE J. Sel. Topics Signal Process.*, vol. 8, no. 5, pp. 876–890, Oct. 2014.

- [21] A. Liu and V. Lau, "Hierarchical interference mitigation for massive MIMO cellular networks," *IEEE Trans. Signal Process.*, vol. 62, no. 18, pp. 4786–4797, Sep. 2014.
- [22] A. Padmanabhan, A. Tölli, and I. Atzeni, "Distributed two-stage multi-cell precoding," in *Proc. IEEE Int. Workshop Signal Process. Adv. in Wireless Commun. (SPAWC)*, Cannes, France, Jul. 2019.
- [23] L. You, X. Gao, X. Xia, N. Ma, and Y. Peng, "Pilot reuse for massive MIMO transmission over spatially correlated Rayleigh fading channels," *IEEE Trans. Wireless Commun.*, vol. 14, no. 6, pp. 3352–3366, Jun. 2015.
- [24] N. N. Moghadam, H. Shokri-Ghadikolaie, G. Fodor, M. Bengtsson, and C. Fischione, "Pilot precoding and combining in multiuser MIMO networks," *IEEE J. Sel. Areas Commun.*, vol. 35, no. 7, pp. 1632–1648, Jul. 2017.
- [25] H. Yin, L. Cottatellucci, D. Gesbert, R. R. Müller, and G. He, "Robust pilot decontamination based on joint angle and power domain discrimination," *IEEE Trans. Signal Process.*, vol. 64, no. 11, pp. 2990–3003, Feb. 2016.
- [26] R. Müller, L. Cottatellucci, and M. Vehkaperä, "Blind pilot decontamination," *IEEE J. Sel. Topics Signal Process.*, vol. 8, no. 5, pp. 773–786, Oct. 2014.
- [27] V. Raghavan, J. H. Kotecha, and A. M. Sayeed, "Why does the Kronecker model result in misleading capacity estimates?" *IEEE Trans. Inf. Theory*, vol. 56, no. 10, pp. 4843–4864, Oct. 2010.
- [28] Y. C. Eldar and A. V. Oppenheim, "Covariance shaping least-squares estimation," *IEEE Trans. Signal Process.*, vol. 51, no. 3, pp. 686–697, Mar. 2003.
- [29] A. K. Hassan, M. Moinuddin, U. M. Al-Saggaf, O. Aldayel, T. N. Davidson, and T. Y. Al-Naffouri, "Performance analysis and joint statistical beamformer design for multi-user MIMO systems," *IEEE Commun. Lett.*, vol. 24, no. 10, pp. 2152–2156, Oct. 2020.
- [30] A. Paulraj, R. Nabar, and D. Gore, *Introduction to Space-Time Wireless Communications*. Cambridge University Press, 2006.
- [31] D. Tse and P. Viswanath, *Fundamentals of wireless communication*. Cambridge University Press, 2005.
- [32] J. Hoydis, S. Ten Brink, and M. Debbah, "Massive MIMO in the UL/DL of cellular networks: How many antennas do we need?" *IEEE J. Sel. Areas Commun.*, vol. 31, no. 2, pp. 160–171, Feb. 2013.
- [33] E. Björnson, J. Hoydis, and L. Sanguinetti, "Massive MIMO networks: Spectral, energy, and hardware efficiency," *Found. Trends Signal Process.*, vol. 11, no. 3–4, pp. 154–655, Jan. 2017.
- [34] L. Grippo and M. Sciandrone, "On the convergence of the block nonlinear Gauss-Seidel method under convex constraints," *Operation Res. Lett.*, vol. 26, no. 3, pp. 127–136, Apr. 2000.
- [35] W. Weichselberger, M. Herdin, H. Özcelik, and E. Bonek, "A stochastic MIMO channel model with joint correlation of both link ends," *IEEE Trans. Wireless Commun.*, vol. 5, no. 1, pp. 90–100, Jan. 2006.
- [36] G. Scutari, F. Facchinei, P. Song, D. P. Palomar, and J.-S. Pang, "Decomposition by partial linearization: Parallel optimization of multi-agent systems," *IEEE Trans. Signal Process.*, vol. 62, no. 3, pp. 641–656, Feb. 2014.
- [37] C. B. Peel, B. M. Hochwald, and A. L. Swindlehurst, "A vector-perturbation technique for near-capacity multiantenna multiuser communication—Part I: Channel inversion and regularization," *IEEE Trans. Commun.*, vol. 53, no. 1, pp. 195–202, Jan. 2005.
- [38] S. Christensen, R. Agarwal, E. Carvalho, and J. Cioffi, "Weighted sum-rate maximization using weighted MMSE for MIMO-BC beamforming design," *IEEE Trans. Wireless Commun.*, vol. 7, no. 12, pp. 4792–4799, Dec. 2008.
- [39] Q. H. Spencer, A. L. Swindlehurst, and M. Haardt, "Zero-forcing methods for downlink spatial multiplexing in multiuser MIMO channels," *IEEE Trans. Signal Process.*, vol. 52, no. 2, pp. 461–471, Feb. 2004.
- [40] A. M. Sayeed, "Deconstructing multiantenna fading channels," *IEEE Trans. Signal Process.*, vol. 50, no. 10, pp. 2563–2579, Oct. 2002.